ADSORPTION OF BORIC ACID ON PURE AND HUMIC ACID COATED AMORPHOUS-ALUMINUM HYDROXIDE: A RAMAN AND XANES SPECTROSCOPY STUDY

A Thesis Submitted to

The College of Graduate Studies and Research

In Partial Fulfillment of the Requirements

For the Degree of

Master of Science

in the

Department of Soil Science

University of Saskatchewan

Saskatoon, Saskatchewan, Canada

By

DANI XU

PERMISSION TO USE

In presenting this thesis in partial fulfillment of the requirements for a Postgraduate degree from the University of Saskatchewan, I agree that the Libraries of this University may make it freely available for inspection. I further agree that permission for copying of this thesis in any manner, in whole or in part, for scholarly purposes may be granted by the professor or professors who supervised my thesis work or, in their absence, by the Head of the Department or the Dean of the College in which my thesis work was done. It is understood that any copying or publication or use of this thesis or parts thereof for financial gain shall not be allowed without my written permission. It is also understood that due recognition shall be given to me and to the University of Saskatchewan in any scholarly use which may be made of any material in my thesis.

Requests for permission to copy or to make other use of material in this thesis in whole or part should be addressed to:

Head of the Department of Soil Science
51 Campus Drive
University of Saskatchewan
Saskatoon, Saskatchewan
Canada, S7N 5A8

ABSTRACT

The fate and mobility of boric acid in the environment is largely controlled by adsorption reactions with soil organic matter and soil minerals to form surface complexes (Marzadori et al., 1991; Su and Suarez, 1995; Yermiyahu et al., 1995; Peak et al., 2002). The effects of humic acid (HA) and dissolved CO_2 on boric acid adsorption on amorphous (am)-$Al(OH)_3$ were investigated as their influence on sorption is potentially important. Although a model system was used in the studies, the findings should be generally useful to better understand the mobility and bioavailability of boric acid in the soil ecosystems.

In this dissertation, boric acid adsorption on pure am-$Al(OH)_3$ and 5% w/w HA coated am-$Al(OH)_3$ were investigated both as a function of pH (4.5 – 11) and initial boric acid concentration (0 – 4.5 mmol L^{-1}). Batch adsorption isotherm experiments were also conducted with samples exposed to atmospheric CO_2 and anaerobic (N_2) conditions to examine the effects of dissolved CO_2 on boric acid adsorption. Both the pH envelope and the adsorption isotherm experiments showed that the HA coating on am-$Al(OH)_3$ and the presence of dissolved CO_2 decreased boric acid adsorption.

Raman spectroscopy and boron (B) *K*-edge X-ray Absorption Near Edge Structure (XANES) spectroscopy were used to investigate the coordination of boric acid adsorbed at mineral/water interfaces. The Raman spectroscopy was less successful than expected as there were difficulties in identifying B bands in the 5% w/w HA coated am-$Al(OH)_3$ samples.

The B *K*-edge XANES spectroscopy yielded better results. The XANES spectra of boric acid adsorption samples showed that both trigonal BO_3 and tetrahedral BO_4 coordinated complexes are present on the pure and HA coated mineral surfaces. At pH 7.0 and 9.2, the adsorption of boric acid on am-$Al(OH)_3$ is predominantly inner-sphere trigonal complexes; with minor amounts of inner-sphere tetrahedral complexes. Both macroscopic and spectroscopic experiments revealed that the combination of HA coating on am-$Al(OH)_3$ and dissolved CO_2 decreased boric acid adsorption compared to adsorption on pure am-$Al(OH)_3$.

The discoveries in this dissertation contribute significantly in understanding the effects of HA and dissolved CO_2 has on boric acid adsorption in the environment. Since B speciation and the stability of am-$Al(OH)_3$ mineral and HA changes with pH, the bioavailability of B is expected to change as well with pH. The adsorption on boric acid on am-$Al(OH)_3$ and/or HA coated am-$Al(OH)_3$ is expected to decrease the amount of boric acid available to plants. Therefore the nutrient management regimen will have to be modified for soils that are high in natural organic matter, carbonate and/or aluminum hydroxyl species.

ACKNOWLEDGEMENTS

I wish to thank Dr. Derek Peak for his support and guidance for the duration of my M.Sc project. I would also like to acknowledge my supervising committee: Drs Fran Walley, P.M. Huang and Ramaswami Sammynaiken for their invaluable advice and assistance for the past two years. I also want to thank my external examiner Dr. Yongfeng Hu for his suggestions and comments as well as his assistance with experimental setup at the Canadian Light Source.

I greatly appreciate the technical help from Dr. Lucia Zuin at the Canadian Light Source with the collection of my XANES data. I also want to thank Dr. Shawn Wettig for his assistance with PZC data collection and Michel Picard (Canadian Museum of Nature) for his gracious donation of the borate mineral samples.

This project was funded by Natural Sciences and Engineering Research Council (NSERC) Discovery Grant, and equipments used in this project were purchased by a Research Tools and Instrument grant from NSERC. The research described in this thesis was performed at the Canadian Light Source, which is supported by NSERC, NRC, CIHR, and the University of Saskatchewan.

I wish to express my gratitude to everyone in the Soil Science Department, in particular Jen Arnold, Pete Burnett, Ailsa Hardie, Jola Pisz and Alexis Schafer. Your friendships and support have made the past two years of my life so much more fun, thanks for the great time!

I want to thank my family and the Degenhardt family for their unconditional love and support. I also want to thank Joe and Josette Khu for their friendship for the past 15 years.

Rory, there is no adequate way to tell you how much I appreciate all your help. Thanks for supporting my academic endeavours.

TABLE OF CONTENTS

LIST OF TABLES

LIST OF FIGURES

1. INTRODUCTION

Boron (B) is an essential micronutrient for plants. The B concentration range between toxicity and deficiency is very narrow. Plants respond primarily to B in soil solution; factors that influence the activity of B in soil solution are: pH, texture, soil organic matter, temperature and moisture content. The knowledge of B coordination on soil constituents such as amorphous (am)-$Al(OH)_3$ and humic acid (HA) coated am-$Al(OH)_3$ would be critical in determining the bioavailability of B in soil solution.

Boron is a trivalent metalloid element (atomic number 5, relative atomic mass 11.81). Its coordination chemistry is one of the most interesting and diverse of any element (Greenwood and Earnshaw, 1984). When a B atom is attached to 3 groups (trigonally coordinated), it is involved in 3 σ bonds, which forms sp^2 hybridization shown in Figure 1.1. When B is tetrahedrally coordinated, sp^3 hybridization occurs (Figure 1.1).

Boron can exist in either 3+ or 1+ oxidation states, but the latter has no relevance in the chemistry of naturally occurring B compounds. The small, highly ionic B^{3+} cation also has little importance under normal conditions. The ionization energies for the valence electrons in B are too great to be compensated by lattice energies of ionic compounds that it might form or by hydration of B^{3+} ion in solution (Cotton and Wilkinson, 1989). Henceforth, B(III) bonding is considered covalent in character.

Many researchers have found a positive correlation between boric acid adsorption and the aluminum hydroxide content of soils (Harada and Tamai, 1968; Bingham et al., 1971). The mechanism of boric acid adsorption on $Al(OH)_3$ is considered to be ligand exchange with reactive surface hydroxyl groups (Sims and Bingham, 1967; McPhail et al., 1972; Goldberg et al., 1993a; Su and Suarez, 1995).

Organic soil constituents such as HA have been recognized to play an important role in the retention of boric acid in soils. Gu and Lowe (1990) found that the boric acid adsorption was highly dependent on pH. Gu and Lowe (1990) proposed that the

observed pH-dependent boric acid adsorption by soil HA is attributable to the different reactivities of boric acid and borate. Furthermore, the differences in adsorptivity between am-$Al(OH)_3$ and HA has never been investigated, therefore the findings from this binary adsorption system study is novel to the field of soil chemistry.

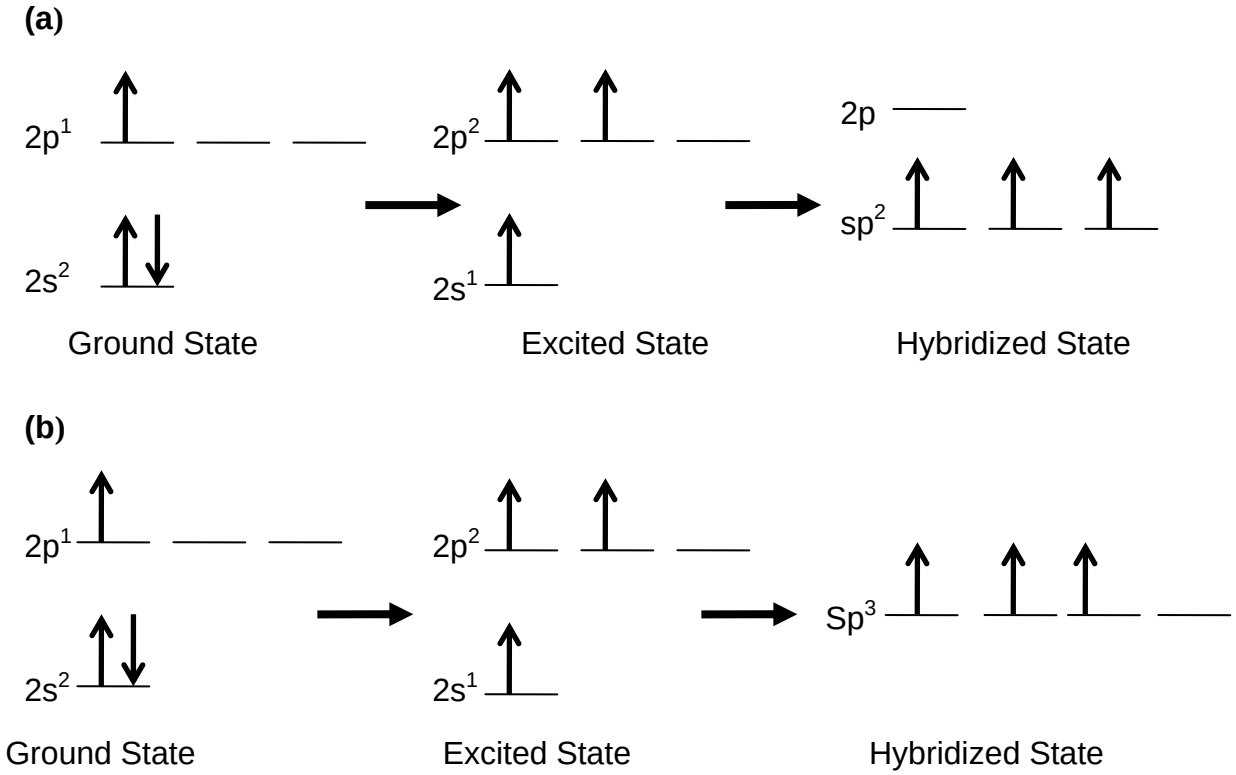

Figure 1.1 Boron molecular orbital diagram for (a) sp^2 (trigonally coordinated boron) versus (b) sp^3 (tetrahedrally coordinated boron) hybrid orbitals.

The adsorption reactions of boric acid at the mineral/water interface leading to the formation of surface complexes was identified as important in controlling the fate and mobility of boric acid in all the above studies. However, the coordination of B in these surface complexes is still not clear as the result of the lack in direct spectroscopic evidence that can precisely determine the presence of trigonal $B(OH)_3$ and/or tetrahedral $B(OH)_4^-$ complexes. Tetrahedral $B(OH)_4^-$ complexes (negatively charged) are likely to be found bound to positively charged mineral surfaces, while trigonal $B(OH)_3$ complexes (neutral in charge) can be easily leached from the soil. Therefore B

bioavailability would be affected dramatically if tetrahedral $B(OH)_4^-$ complexes can form under normal soil pH.

The objective of this study was to investigate the coordination of adsorbed boric acid on am-$Al(OH)_3$ and 5% w/w HA coated am-$Al(OH)_3$ surfaces as a function of pH and boric acid concentration. The experimental approach for the present study is to combine macroscopic adsorption experiments with molecular-scale spectroscopic techniques to investigate boric acid reactions under natural conditions.

2. LITERATURE REVIEW

2.1. Aqueous Chemistry of Boron

Since B does not undergo reduction/oxidation reactions or volatilization under normal environmental conditions, the chemistry of monomeric B involves simple acid/base reactions. At low concentration, B exists as monomeric boric acid $B(OH)_3$ and borate $B(OH)_4^-$ (Cotton and Wilkinson, 1989). The trigonal planar (sp^2 hybridized) boric acid molecule with an empty 2*p* atomic orbital behaves as a Lewis acid, accepting an electron to form its conjugate base, a tetrahedral (sp^3 hybridized) borate anion (Figure 2.1). The negative log of the first acidity constant (pK_a) for this reaction is approximately 9.25 (Equation 2.1) (Shriver and Atkins, 1994).

$$B(OH)_3 + 2H_2O \leftrightarrow B(OH)_4^- + H_3O^+ \qquad pK_a = 9.25 \qquad (2.1)$$

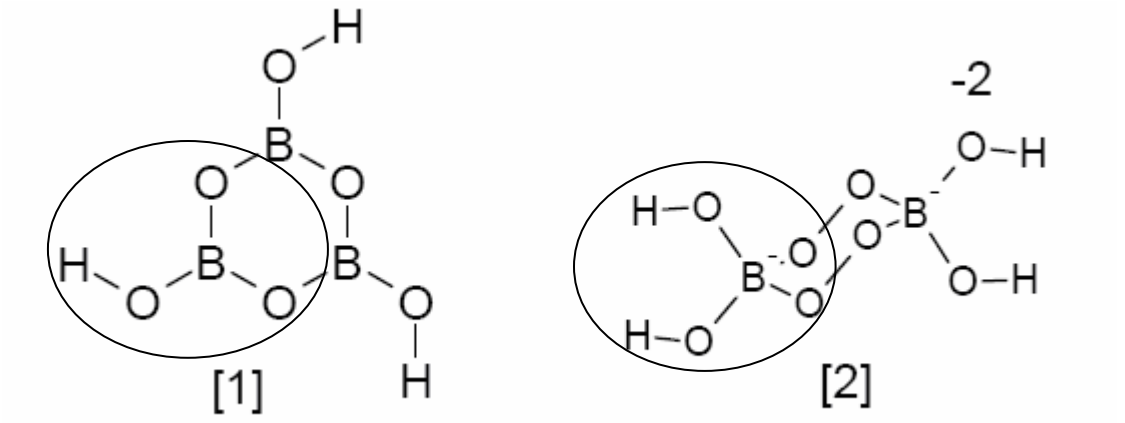

Figure 2.1 All the B and O atoms in metaboric acid [1] are sp^2 hybridized. All the B and O in peroxoborate anion [2] are sp^3 hybridized. The B center in metaboric acid resembles boric acid which is trigonal planar shaped, and the B center in peroxoborate resembles the borate anion, the conjugate base of boric acid, which is tetrahedral shaped.

Cryoscopic methods, nuclear magnetic resonance, IR, conductance, pH titration and temperature jump techniques have established the presence and structure of polyborate ions in solution. Extensive work done by Drs. Ingri and Mesmer (Discussed in Maya, 1976) postulated a set of numbers that provided both the number of B atoms and the charge for different polyborate ions. Interactions between $B(OH)_3$ and $B(OH)_4^-$ species may form polyborate ions at B concentrations greater than 25 mmol L^{-1} (Cotton and Wilkinson, 1989). These polyborate ions include $B_3O_3(OH)_4^-$ (Equation 2.2), $B_4O_5(OH)_4^{2-}$ (Equation 2.3), $B_5O_6(OH)_4^-$ (Equation 2.4), as well as ones that incorporate B_3O_3 rings in the structure (Equation 2.5).

$$2B(OH)_3 + B(OH)_4^- \leftrightarrow B_3O_3(OH)_4^- + 3H_2O \quad (2.2)$$

$$2B(OH)_3 + 2B(OH)_4^- \leftrightarrow B_4O_5(OH)_4^{2-} + 5H_2O \quad (2.3)$$

$$4B(OH)_3 + B(OH)_4^- \leftrightarrow B_5O_6(OH)_4^- + 6H_2O \quad (2.4)$$

$$B(OH)_3 + 2B(OH)_4^- \leftrightarrow [B_3O_3(OH)_5]^{2-} + 3H_2O \quad (2.5)$$

2.2. Sources of Boron in the Environment

The United States and Turkey are the world's largest producers of B. Boron does not appear in nature in its elemental form but is commonly found in borax, boric acid, colemanite, kernite, tourmaline, ulexite and borate minerals. Boron is widely distributed in both the lithosphere and hydrosphere. In the earth's crust, the concentration of B averages about 10 mg kg^{-1} (Krauskopf, 1972). In sea water, it can range from 1-10 mg B kg^{-1}, and the concentration in river water is about 1/350 of that in sea water (Morgan, 1980). The level of B in common rocks and clay is shown in Table 2.1. Soils may be divided into two types: those with low B content (<10 mg B kg^{-1}) likely derived from igneous and metamorphic rocks and those with high B content (10-100 mg B kg^{-1}) likely to have originated from marine shale parent material. Most soils have low B content, while some have been found to contain over 200 mg B kg^{-1} (Morgan, 1980).

2.2.1. Boron in Plants

Boron is one of several essential micronutrients required by plants at low levels. Boron is thought to be important during development and the structural integrity of dicotyledonous plant cell walls as it plays a primary role in the biosynthesis of lignin (Ascerbo et al., 1973). Boron is also vital in protecting cell membranes against damage

Table 2.1 Level of boron in common rock type and phyllosilicates (adapted from (Krauskopf, 1972; Spiers et al., 1983).

Class of rock/mineral	**Type of rock/mineral**	**Concentration (mg kg^{-1})**
Igneous	Granite	15
	Basalt	5
Metamorphic	Limestone	20
Sedimentary	Sandstone	35
	Shale	100
Clay minerals	Muscovite	10-500
	Biotite	1-6
	Illite	100-2000 or greater
	Montmorillonite	5-200
	Kaolinite	10-30
	Chlorite	50 or lower
Level of boron found in soil		**2-100**

from phenolic compounds and is required during pollen germination and pollen tube growth (Parr and Loughman, 1983). The labile fraction of B (mostly mononuclear species of boric acid and borate) are available for plant to utilize; these two species account for only 10% of total soil B content (Xu et al., 2001).

Boron deficiencies are widespread, and have been reported in 80 countries and for 132 crops in the last 60 years (Shorrocks, 1997). Boron deficiency is usually associated with either coarse textured soils in humid regions, which can lead to B leaching, or the liming of acid soils, which can raise soil pH and subsequently decrease B solubility making it less available for plant uptake (Reisenauer et al., 1973).

Conversely, if B is present in excessive amounts, it limits plant growth through stem dieback, leaf necrosis, and disruption of chloroplast membranes (El-Motaium et al., 1994). Phytotoxic levels of B are often associated with semi-arid and arid areas where

the soil is naturally rich in B, or when B laden irrigation water is applied to the soil (Keren and Bingham, 1985). The application of surface mining wastes and fly ash to soil could also contribute to high B concentration (Nable et al., 1997).

2.2.2. Boron in Soil

There are different forms of B that can exist within the soil, such as the nearly insoluble mineral deposits in the form of tourmaline micas or B bound tightly within the clay structures. Other examples B found in soil are the partially labile B adsorbed on clay surfaces and edges or on other hydroxylated mineral surfaces, as well as B that are complexed to soil organic matter (SOM) (Goldberg, 1997). The overall amount of B available to plants will depend upon the weathering of nearly insoluble B mineral reserves. However, on a smaller time-scale, plants have to rely on B released from hydroxylated mineral surfaces and SOM. The speed at which B is released will likely control B availability.

Boron in soil solution exists principally as boric acid and the borate anion, which could be complexed through *cis*-diol linkages to small soluble organic molecules (Figure 2.2). Under normal soil pH, between pH 5 to 8.5 (Baas Becking et al., 1960), the amount of B presents in the form of the borate anion is likely to be minimal.

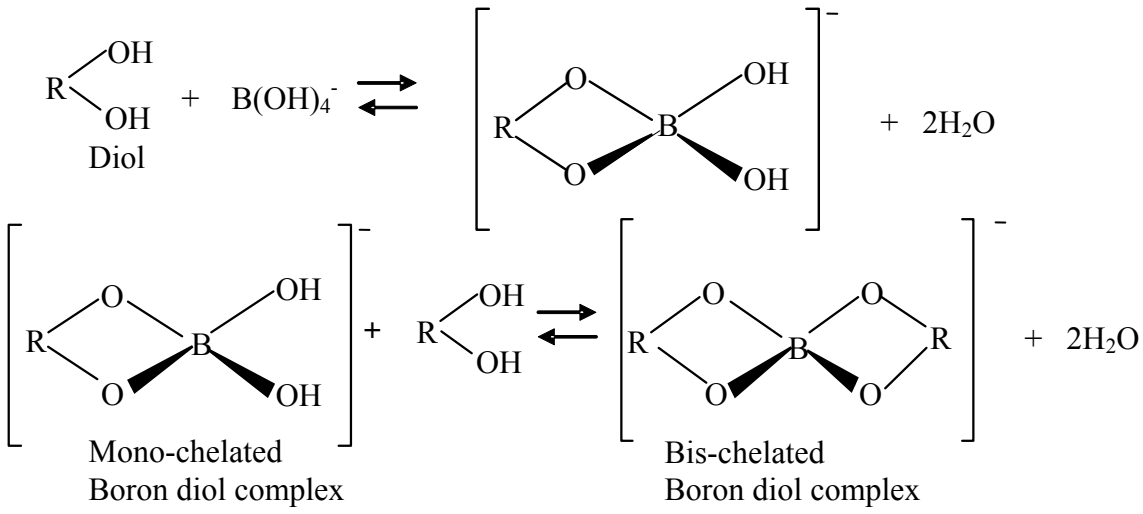

Figure 2.2 Formation of B-diol complexes, modified from Huettl (1976).

Since the method was first proposed by Berger and Troug (1939), the determination of the quantities of B extracted by hot water has been widely used as a measure of plant available B in soil. There have been other extractants proposed, such as phosphoric and hydrofluoric acids, but none have shown sufficient benefits over hot water extraction to warrant its replacement.

2.3. Factors Affecting Boric Acid Adsorption

Since the most important B species in the soil are boric acid and its conjugate base borate, which from now on will be collectively denoted as boric acid, the next section will discuss in detail on factors that affect their adsorption in soil.

2.3.1. pH

The relationship between boric acid concentration and pH has been the focus of many previous studies elucidating the behaviour of boric acid in an aqueous environment (Olson and Berger, 1946; Huettl, 1976; Keren and Sparks, 1994). The concentration of boric acid in soil is significantly correlated with solution pH, thus making pH one of the most important factors in controlling the amount of boric acid available to plant (Berger and Truog, 1939; Elrashidi and O'Connor, 1982) . Boric acid adsorption pH envelope resembles a bell-shaped curve. Between pH 3 and 9, boric acid adsorption increases as a function of solution pH (Bingham et al., 1971; Schalscha et al., 1973; Keren and Mezuman, 1981; Keren et al., 1985; Barrow, 1989; Lehto, 1995). Conversely, between pH 10 and 11.5, boric acid adsorption decreases as a function of solution pH (Goldberg and Glaubig, 1986a).

2.3.2. Soil Texture

The amount of labile boric acid is thought to be dependent on soil pH as well as soil texture, as coarse textured soils often contain less available boric acid than fine textured soils (Gupta, 1968; Fleming, 1980). Elrashidi and O'Connor (1982) found a significant positive correlation between native boric acid and soil clay content. At the same time, other researchers have also found adsorbed boric acid increases with

increasing soil content of clay minerals such as kaolinite, montmorillonite and chlorite (Bhatnagar et al., 1979; Wild and Mazaheri, 1979; Keren and Mezuman, 1981).

2.3.3. Ionic Strength

Keren and O'Connon (1982) studied the adsorption of boric acid on illite and montmorillonite under the presence of a divalent cation ($CaCl_2$) and a monovalent cation (NaCl) solution. Under high pH, boric acid adsorption on the montmorillonite was limited by the negative charge on the clay's interlayer space. At increased ionic strength, divalent cations were better than monovalent cations at reducing the negative charge of the interlayer space through non-specific adsorption, thus boric acid adsorbed more readily. For Kaolinite (1:1) clay, boric acid adsorption was less affected by ionic strength, due to the lack of interlayer spacing, which reduces the number of pH dependent charges.

2.3.4. Soil Organic Matter

Soil organic matter is known to play an important role in the ecosystem, particularly in all physical, chemical and biological processes. Furthermore, it is an integral part of metal mobility and speciation, inorganic and organic contaminant transport, nutrient availability, and soil buffering capacity (Sposito, 1989).

Soil organic matter is regarded as an important factor in determining the amount of boric acid adsorption to soils. Early studies conducted by Olson and Berger (1946) discovered that the destruction of SOM by oxidation led to substantial release of boric acid, and a slight decrease in boric acid fixation. Parks and White (1952) also showed that the affinity between humic substances and boric acid is significant. Gupta (1968) and Elrashidi and O'Connor (1982) have also determined a positive relationship between SOM content and boric acid content in soil.

Soil organic matter is composed of particulate organic matter (POM $\geq$ 1.0 μm), colloidal organic matter (0.22 μm $\leq$ COM $\leq$ 1.0 μm), and dissolved organic matter (DOM < 0.22 μm) (Tombacz et al., 1997). The high functionality of DOM is largely due to the humic and fulvic acid content, which contributes numerous carboxylic acids (COOH) and phenolic (OH) functional groups for boric acid adsorption. However, the

mechanism of boric acid adsorption to humic and fulvic acid is still unclear. Yermiyaho et al. (1988) proposed ligand exchange as a possible mechanism for boric acid sorption by organic matter. Parks and White (1952) speculated the formation of boric acid-diol complexes following the breakdown of SOM, while Huettl (1976) speculated that α-hydroxyl carboxylic acid groups may account for boric acid adsorption to SOM. The high nitrogen component (amino acids, purines, pyrimidines and heterocyclic) of soil organic matter may also have been overlooked as a source of boric acid complexation.

2.3.5. Temperature and Moisture Content

Boric acid adsorption has a positive correlation with soil temperature. This relationship could be explained by the combined effect of soil temperature and soil moisture. Boron deficiency is associated with dry summer conditions, when plants encounter less available B when they are forced to extract moisture from greater depths (Fleming, 1980). Between 10 – 40 °C, B adsorption decreased as a function of temperature in soils that contain predominantly crystalline minerals (Biggar and Fireman, 1960; Goldberg et al., 1993b); the trend is reversed in amorphous soils (Bingham et al., 1971).

2.4. Interaction of Boron with Soil Constituents

2.4.1. Adsorption Mechanisms and Surface Complexation Models

Sorption is a general term used to describe the retention mechanism at any surface (Sparks, 2003). Three types of sorption mechanisms are of interest: adsorption, surface precipitation and polymerization. Adsorption is the process through which a net accumulation of a compound occurs at the solid/aqueous interface (Sparks, 2003), it includes both dissolution and desorption. Unlike mononuclear adsorption, surface precipitation forms a three-dimensional phase on the surface that can arise from polymeric metal complexes, aqueous polymers or nucleation of homogenous species due to saturation (Chrisholm-Brause et al., 1990). Polymerization is the formation of multinuclear species that are soluble in solution (Sparks, 2003).

There are two types of adsorption reactions that can occur between an aqueous ion and particle surfaces: 1) inner-sphere complexation (or ligand exchange reaction)

that involves direct binding of the species to the surface and, 2) outer-sphere complexation, which involves binding of species through their hydration shell. Possible molecular configurations of boric acid inner-sphere monomeric complexes of boric acid with mineral surfaces are shown in Figure 2.3.

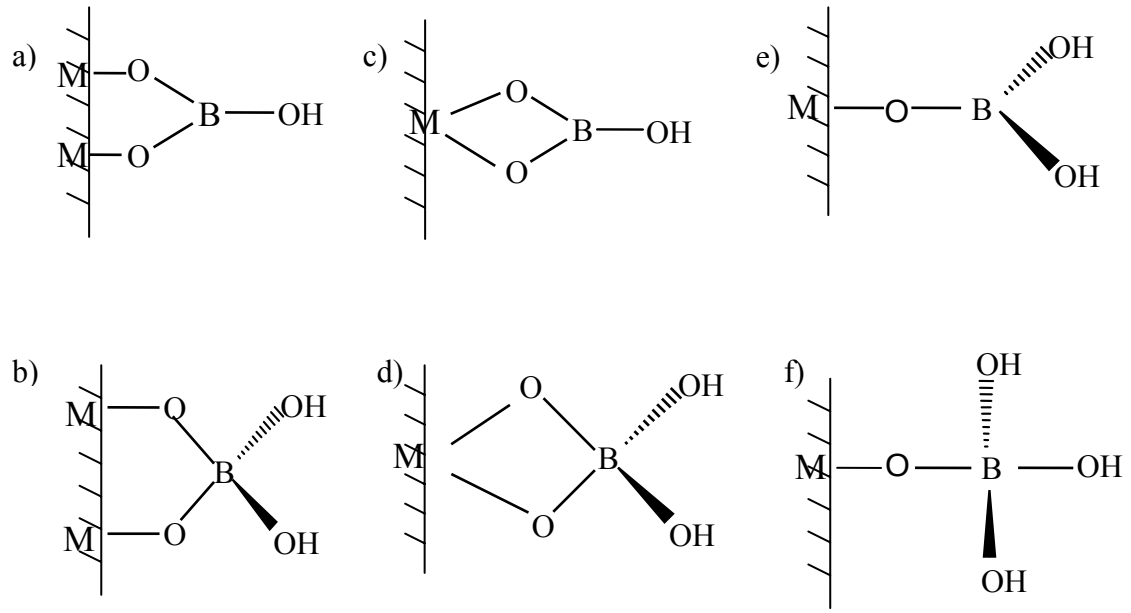

Figure 2.3 Possible Molecular configurations of $B(OH)_3$ and $B(OH)_4^-$ inner-sphere monomeric complexes of B with mineral surfaces. M represents a metal cation, either Al or Fe. a) boric acid bidentate binuclear; b) borate bidentate binuclear; c) boric acid bidentate mononuclear; d) borate bidentate mononuclear; e) boric acid monodentate mononuclear; f) borate monodentate mononuclear. Adapted from Peak et al. (2002).

Inner- and outer-sphere complexes can be distinguished by studying the effects of ionic strength on ion adsorption. McBride (1997) explained the ionic strength effect using mass action principle. He suggested that the ions forming inner-sphere surface complexes exhibit ionic strength dependent adsorption, which increases in magnitude with the increase in ionic strength. The increase in specific ion adsorption is the result of increased solution activity of the counter ion of the background electrolyte, which is available to compensate the surface charge generated by specific ion adsorption.

Surface complexation models, such as the constant capacitance model and the triple layer model, have been documented to describe boric acid adsorption on various

aluminum (Al) and iron (Fe) oxides, clay minerals, and soils (Goldberg and Glaubig, 1985; Goldberg and Glaubig, 1986a; Goldberg and Glaubig, 1986b; Goldberg et al., 1993a; Goldberg, 1999; Goldberg et al., 2004). The constant capacitance model has been more accurate in describing systems undergoing ligand exchange reactions because it considers all ions to have adsorbed and formed inner-sphere complexes, whereas the triple layer model considers both inner-sphere and outer-sphere complexes. The latest research by Goldberg (2005) concluded that the triple layer model was best to describe boric acid adsorption on Al and Fe oxides, kaolinite, montmorillonite, and two soils simultaneously both as a function of solution pH and solution ionic strength. In systems where boric acid adsorption is known to be ionic strength independent, the constant capacitance model should be used in place of the triple layer model because of the simplicity of the constant capacitance model (Goldberg, 2005).

2.4.2. Interaction of Boric Acid with Aluminum phases

Many researchers have found a positive correlation between boric acid adsorption and the Al oxide content of soils (Harada and Tamai, 1968; Bingham et al., 1971). Boric acid adsorption on both crystalline and amorphous Al oxide increased with increasing pH up to an adsorption maximum between pH 6 to 8 (Sims and Bingham, 1968; McPhail et al., 1972; Goldberg and Glaubig, 1985; Su and Suarez, 1995). After reaching the maximum, boric acid adsorption decreases with increasing pH. Hatcher et al. (1967) and Sims and Bingham (1968) have found that boric acid adsorption was greatest on freshly precipitated minerals and the adsorptivity decreases as minerals become more crystalline due to aging. On a per mass basis, boric acid adsorption is much greater on Al oxide than on Fe oxide (Sims and Bingham, 1968; Goldberg and Glaubig, 1985). Goldberg and Glaubig (1985) credits that fact to the higher surface area of aluminum oxides, as they found the adsorption on a per square meter basis were quite comparable for the two oxides. Boric acid adsorption on Al oxide generally completes after 24h reaction time, making it a relatively fast reaction (Choi and Chen, 1979).

The mechanism of boric acid adsorption on Al oxide mineral is considered to be ligand exchange with reactive surface hydroxyl groups (Sims and Bingham, 1967; McPhail et al., 1972; Goldberg et al., 1993a; Su and Suarez, 1995). Ligand exchange

mechanism is often characterized by a shift in the point of zero charge (PZC) of the mineral as the adsorbent become specifically adsorbed on mineral surface. Boric acid adsorption has been documented to shift the PZC to a more acidic pH value (Beyrouty et al., 1984; Goldberg et al., 1993a; Su and Suarez, 1995).

2.4.3. Interaction of Boron with Iron Phases

Elrashidi and O'Connor (1982) discover that %w/w Fe oxide content was a significant variable in multiple regression equations explaining the inconsistency in adsorbed boric acid, soluble boric acid and total boric acid for soils. Boric acid's adsorptive behaviour on Fe oxide is akin to its behaviour on Al oxide. The adsorption of boric acid on Fe oxides increased with increasing pH up to an adsorption maximum at pH 7 to 9 (Bloesch et al., 1987). Beyond pH 9, boric acid adsorption decreased with increasing pH. Similar to B adsorption on Al oxide, the greatest adsorption was found on freshly prepared minerals (Sims and Bingham, 1968) and the adsorption reaction on Fe oxide also completes within 24 h (Choi and Chen, 1979).

2.4.4. Interaction of Boron with Clay Minerals

Much research has been devoted to the study of layer silicate clay mineral as boric acid adsorbing surfaces in soils (Hingston, 1964; Fleet, 1965; Porrenga, 1967; Sims and Bingham, 1967; Couch and Grim, 1968; Sims and Bingham, 1968; Singh, 1971; Jasmund and Lindner, 1973; Keren and Gast, 1981; Keren et al., 1981; Keren and Mezuman, 1981; Keren and O'Connon, 1982; Keren and Talpaz, 1984; Mattigod et al., 1985; Goldberg and Glaubig, 1986b; Goldberg et al., 1993a; Goldberg et al., 1993b; Keren et al., 1994; Keren and Sparks, 1994; Goldberg et al., 1996). Boric acid adsorption on layer silicate clay minerals exhibits similar trends to its adsorption on metal oxide surfaces. Increasing boric acid adsorption occurs with increasing pH until reaching the adsorption maximum between pH 8 and 10 (Hingston, 1964; Sims and Bingham, 1967; Mattigod et al., 1985). As pH increases beyond the maximum, boric acid adsorption declines sharply. Many researchers have found the trend for boric acid adsorption on clay mineral to be: kaolinite < montmorillonite < illite (Hingston, 1964; Sims and Bingham, 1967; Jasmund and Lindner, 1973; Keren and Mezuman, 1981).

Keren and Mezuman (1981) found that at concentration below 2.5 mmol L^{-1}, adsorption of clay follows the Langmuir equation shown in Equation 2.6.

$$c/x=1/bK+c/b \quad (2.6)$$

Where, c = concentration of B at equilibrium in mmol L^{-1}, b = maximum adsorption parameter, K = relative rates of adsorption and desorption at equilibrium and x = B adsorbed per mass of adsorbent.

2.4.5. Interaction of Boron with Humic Acid

Organic soil constituents such as HA have been recognized to play an important role in the retention of boric acid in soils. Gu and Lowe (1990) attempted to elucidate the role of HA as they examined boric acid adsorption on HA isolated from three British Columbia soils. They found that the boric acid adsorption was highly dependent on pH. The amount of boric acid adsorbed by HA increased very slowly up to about pH 6, but increased significantly with further pH increase. The adsorption maximum occurred around pH 9.2, with further pH increases leading to a rapid decline in boric acid adsorption. This pattern of pH isotherm is similar to that observed for clay minerals, Al and Fe oxides. Gu and Lowe (1990) suspect that the observed pH-dependent boric acid adsorption by soil HA is attributable to the different reactivity of boric acid and borate. At pH below 7, they suspect most adsorption is the result of the interaction between boric acid and α-hydroxyl-carboxyl groups of HA. Over the pH range 7.5 – 9.5, they anticipate that anionic form borate would increase in abundance as pH increases, as borate has a strong affinity for *cis*-diol sites. Above pH 9.5, the increase in OH^- activity would compete for the borate adsorption sites, resulting in a decrease in boric acid adsorption. Overall the researchers suspect that in neutral soils with organic matter contents <5%, the contribution of HA to boric acid adsorption is likely to be minor, especially when large amounts of Al and Fe oxides are present (Gu and Lowe, 1990).

2.4.6. Interaction with other ions

The soil solution is a diverse matrix that contains various other ions that may complex with boric acid. Gupta and MacLeod (1977) found if B fertilizer is applied, the amount of uptake by plants is correlated to the availability of calcium or magnesium. Gupta (1993) also found nitrogen and sulphur application can lead to a decrease in plant boric acid uptake or even B deficiencies. A significant relationship between the availability of boric acid and potassium has also been discovered by Woodruff et al. (1987). They showed that B deficiency may be exacerbated when heavy application of potassium is applied. Phosphorus and B interaction has also been reported by Bloesch et al. (1987), they found that the presence of phosphate competes for the same adsorption site as borate on Al hydroxide surfaces, which could explain decreased boric acid adsorption in the presence of phosphorus.

2.5. Occurrence, Formation and Properties of Amorphous Aluminum Hydroxide in Soils

2.5.1. Occurrence and Formation of Amorphous Aluminum Hydroxide in Soils

Despite being the third most abundant element on the Earth's curst, only a few crystalline Al oxides, hydroxide or oxyhydroxides are found, and only one of them, gibbsite, is commonly found in soils. Gibbsite, bayerite, nordstrandite and Doyleite are polymorphs of $Al(OH)_3$ (Table 2.2). They all have the same dioctahedral $Al(OH)_3$ sheet-like structure. Gibbsite has one-half of its hydroxyls oriented perpendicular to the octahedral sheets, and the other half is pointed towards the empty octahedral sites (Figure 2.4), which results in a neutral sheet. The lack of a charge on the gibbsite sheets means that there is no charge to retain ions between the sheets and keep the sheets together. Therefore the sheets are only held together by weak residual bonds, thus creating a very soft, easily cleaved mineral (Schulze, 2002).

Aluminum exists as $Al(H_2O)_6^{3+}$ ion in aqueous solutions, it could undergo hydrolysis to form several other soluble species (Equation 2.7, 2.8, 2.9 and 2.10) written without H_2O molecules) (Huang, 1988; Huang, 1991). Below pH 3, $Al(H_2O)_6^{3+}$ is the dominant Al species, but as pH increases the speciation shifts dominance to $Al(OH)^{2+}$,

Table 2.2 Various chemical compositions of aluminum hydroxide, aluminum-oxyhydroxide and aluminum-oxide minerals.

Mineral	Chemical Composition
Gibbsite†	$Al(OH)_3$
Bayerite	$Al(OH)_3$
Nordstrandite	$Al(OH)_3$
Doyleite	$Al(OH)_3$
Boehmite	AlOOH
Diaspore	AlOOH
Corundum	Al_2O_3

†mineral that occurs most frequently in soils.

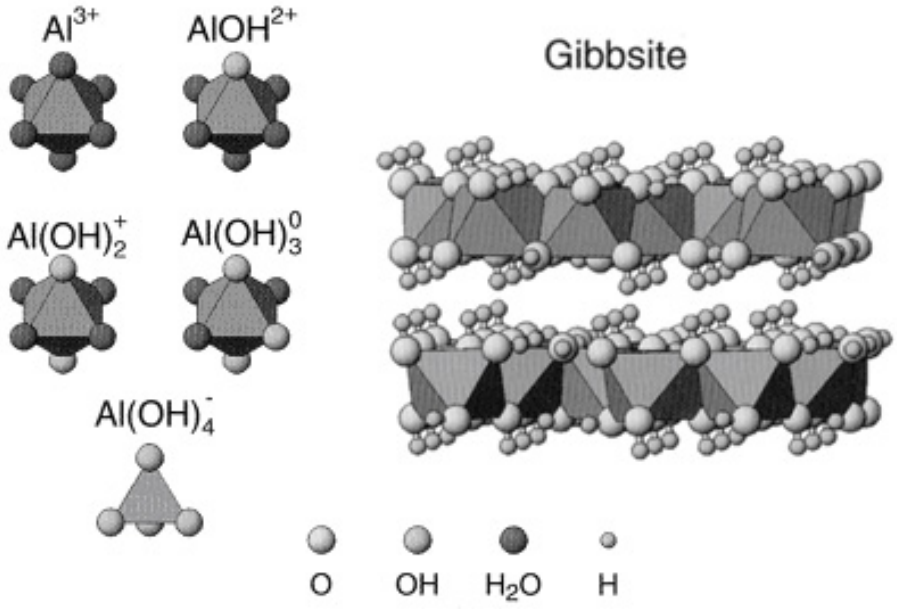

Figure 2.4 Polyhedral models of the crystal structure of gibbsite, and five monomeric aluminum solution species. Modified from Huang et al. (2002).

$Al(OH)_2^+$, $Al(OH)_3$ and $Al(OH)_4^-$. Above pH 6.5, $Al(OH)_4^-$ is the predominant ion in solution (Figure 2.5).

$$Al(H_2O)_6^{3+} \leftrightarrow Al(OH)^{2+} + 5H_2O + H^+ \quad (2.7)$$

$$Al(H_2O)_6^{3+} \leftrightarrow Al(OH)_2^+ + 4H_2O + 2H^+ \quad (2.8)$$

$$Al(H_2O)_6^{3+} \leftrightarrow Al(OH)_3 + 3H_2O + 3H^+ \quad (2.9)$$

$$Al(H_2O)_6^{3+} \leftrightarrow Al(OH)_4^- + 2H_2O + 4H^+ \quad (2.10)$$

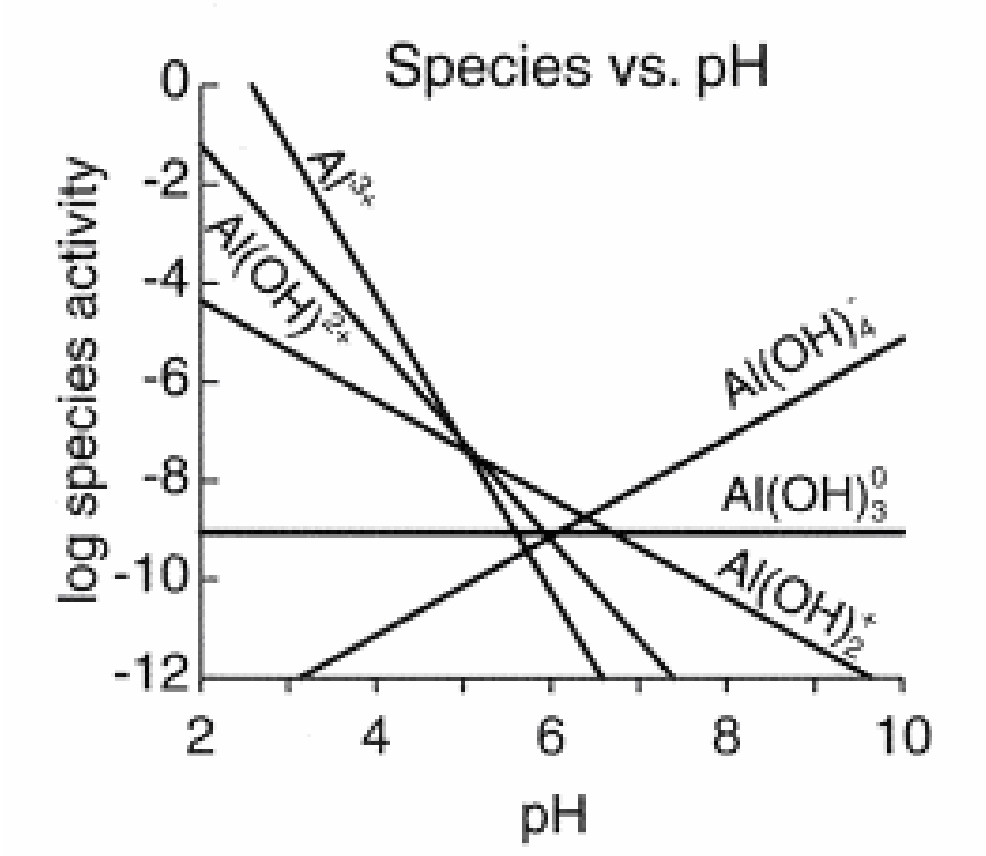

Figure 2.5 Distribution of activities of the monomeric solution species as a function of pH, calculated based on equilibrium with gibbsite and using stability constants modified from Bertsch and Parker (1996).

With increasing pH, these monomeric hydrolysis species will polymerize to form hydroxyl-Al polymers. These polymers will expand in size and their net surface charge will no longer be able to maintain a stable colloidal system, prompting precipitates to form (Hsu, 1989). Factors such as rate of hydrolysis, temperature and Al/OH molar ratio can have a profound influence on the characteristics of the precipitate.

Various synthesis methods of am-$Al(OH)_3$ minerals have been published (Sims and Bingham, 1968; McPhail et al., 1972; Goldberg et al., 2001), and the surface area of these amorphous minerals differs depending on the method employed. Goldberg et al. (2001) attribute the differences in surface area of am-$Al(OH)_3$ to the differences in preparation methods, especially the concentration of starting reagents. By keeping the concentrations of starting reagents ($AlCl_3$ and NaOH) under one molar and maintaining

the Al : OH molar ratio at a value of 0.375, Goldberg et al. (2001) were not only able to attain a relatively high surface area mineral but the surface area remained stable over time.

2.5.2. Properties of Amorphous Aluminum Hydroxide in Soils

Chemical properties such as cation and anion exchange capacities (CEC and AEC) of $Al(OH)_3$ vary with pH, crystallinity, surface area, adsorbate and methods of measurement. For crystalline $Al(OH)_3$ such as gibbsite, the CEC and AEC are 1 cmol kg^{-1} and 3 cmol kg^{-1}, respectively (van Raij and Peech, 1972). The same properties are generally one to two orders of magnitude greater in am-$Al(OH)_3$ (Kwong and Huang, 1979).

Ligand exchange of oxyanions (NO_3^-, SO_4^{2-}, PO_4^{3-}, SeO_3^{3-} and BO_4^-) with the surface hydroxyl groups and protonated hydroxyls on hydrous metal oxides is the accepted mechanism of adsorption for am-$Al(OH)_3$ minerals (Huang, 1988). Humic acid adsorbs to $Al(OH)_3$ by ligand exchange on edge sites in neutral and high pH, while additional adsorption was seen at lower pH by H bonding to the un-reactive planar faces (Huang et al., 2002). Competition for sorption sites between organic matter and oxyanions has been documented on gibbsite surfaces (Afif et al., 1995). Despite the small occurrence of amorphous Al in the environment, am-$Al(OH)_3$ can still account for a high level of oxyanion adsorption in the environment due to its large surface area.

2.6. Occurrence, Formation and Properties of Humic Acids in Soils

2.6.1. Occurrence and Formation of Humic Acids in Soils

Berzelius, the forefather of humic substances research, was the first to separate humic matter into three components. They are 1) HA, which is soluble in alkaline solution, 2) humine, which is insoluble in alkaline solutions and 3) fulvic acid, which is soluble in alkaline, neutral and acidic conditions.

Humic acid is the most widely studied humic compound in soils. The theory behind HA formation has been debated over the last 100 years. The formation of HA is hypothesized to have occurred by one of the following pathways (Figure 2.6).

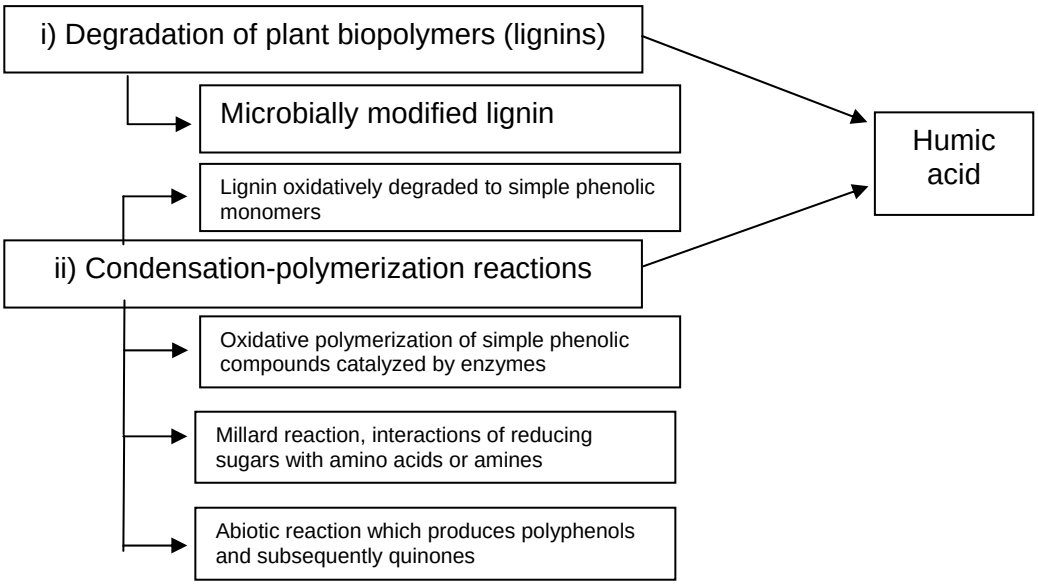

Figure 2.6 Synthesis pathway of HA, modified from Schnitzer and Schulten (1998).

Over the years there have been numerous chemical structures proposed for HA, however, none of the structures proposed thus far have been accepted as representative HA structures. The chemical composition of HA varies according to the source, but generally falls within the ranges: 50-60% carbon; 30-35% oxygen; 4-6% hydrogen; 2-4% nitrogen and 0-2% sulphur (Schnitzer and Schulten, 1998). The structure of HA has been described to contain units similar to a number of smaller, aromatic organic acids, such as benzoic, salicylic, phthalic, 3-hydroxybenzoic, protocatechuric, 3-hydrocycinnamic, caffeic, ferulic, gallic, tannic and vanillic acids. It has been suggested that the predominant proton binding sites on HA may be comparable to the simple organic ligands *o*-phthalate and or salicylate (Schnitzer, 1965; Schnitzer and Skinner, 1965; Reuter and Perdue, 1977; Marinsky et al., 1982; Perdue, 1988). It is most likely that the carboxylic (-COOH) and phenolic (-OH) groups on the organic acid are responsible for the majority of cation adsorption, however it's difficult to pinpoint the exact binding site in each HA sample. Furthermore, the HA may change structural configuration as a function of pH, ionic strength and concentration of adsorbate, therefore one can only speculate on the type of bonding mechanism that occurs with HA.

2.6.2. Properties of Humic Acids in Soils

One of the most fundamental reactions in soils is thought to be between HA and hydrous oxides of Fe and Al and clay minerals. These reactions are believed to occur via O-containing functional groups such as COOH and phenolic OH groups in HA, with metals and minerals. The first step in most of these reactions is the dissociation of the H at the end of COOH and OH groups, which is governed by pH and the dissociation constant of the functional groups involved.

2.6.3. Limitations in the Use of Commercial Humic Acids in Soil Research

Extraction and isolation of HA from soils are time-consuming and arduous processes. In addition to the extensive time and labour requirements, specialized equipment and chemicals are necessary to isolate humic substances (Swift, 1996). For these reasons, many researchers have used commercially available HA in their experiments. One of the major drawbacks in working with commercial HA is the lack of information on its origin and the methods of extraction. Consequently, that makes it nearly impossible for researchers to attach any of site specific data when using these materials.

A review conducted by Malcolm and MacCarthy (1986) found the organic matter in commercial HA is uniform in nature and the Aldrich humic acid sodium salt, the commercial HA chosen for this thesis, is similar to Wyoming dopplerite.

2.7. Experimental Approaches

2.7.1. Point of Zero Charge

The charging of metal hydroxides is very important in determining the adsorption behaviour of ions on these surfaces. The surface charge of metal hydroxides can be positive, zero or negative. This variable charge on metal surfaces can be influenced by the adsorption and desorption reactions of protons on the surface groups of the metal hydroxide.

Zeta potential is a measure of the magnitude of the repulsion or attraction between particles. The point where the plot of zeta potential versus pH passes through zero zeta potential is called the isoelectric point (Figure 2.7) (Hunter, 1988). The

Zetasizer Nano series calculates the zeta potential by determining the electrophoretic mobility and then applying it to the Henry equation (Equation 2.11). Electrophoretic mobility is obtained by performing an electrophoresis experiment on the sample and

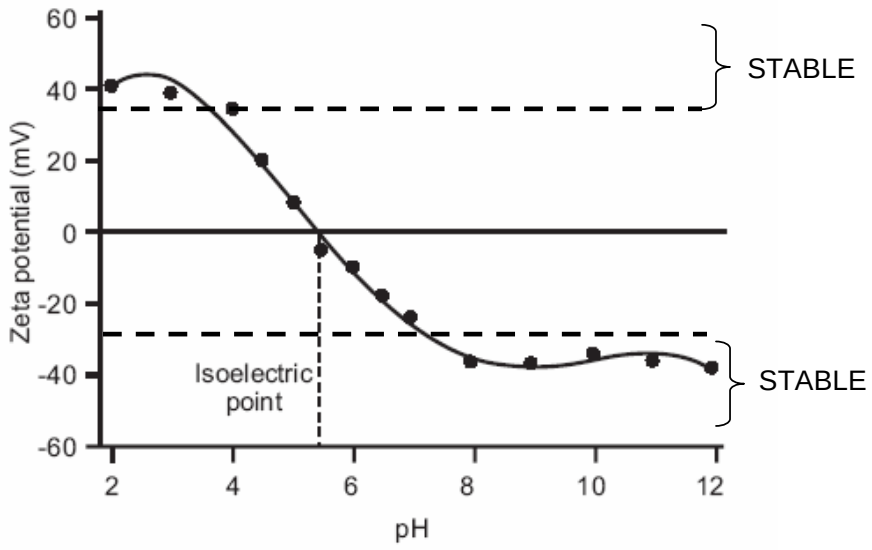

Figure 2.7 A typical plot of zeta potential versus pH is shown. Modified from Hunter (1981).

measuring the velocity of the particles using Laser Doppler Velocimetry. Electrophoresis is the application of an electric field across an electrolyte resulting in the charged particles suspended in the electrolyte moving at a constant velocity towards the electrode of opposite charge. The velocity of the particle, commonly referred to as its electrophoretic mobility, is dependent on the zeta potential. With the knowledge of electrophoretic mobility the Henry equation can then be applied to determine the zeta potential.

$$U_E = (2\varepsilon\zeta / 3\eta) \cdot f_1(\kappa a) \qquad (2.11)$$

Where ζ is zeta potential, U_E is electrophoretic mobility, ε is Dielectric constant, η is viscosity and $f_1(\kappa a)$ is the Henry's function. $f_1(\kappa a)$ in this case is 1.5 and is referred to as the Smoluchowski approximation, which is a formula which relates the electrophoretic mobility of a rigid colloidal particle moving in an aqueous media.

2.7.2. pH Envelopes

Adsorption edge refers to the narrow pH range where sorption increases to nearly 100% (Sparks, 2003), since the adsorption of boric acid is pH-dependent, it's relevant to conduct wet chemistry experiments to derive the pH where the adsorption edge occurs. Often the pH of the adsorption edge is related to the pKa of adsorbate. These experiments are conducted by varying the pH of an adsorptive solution of a known concentration and volume and bring it to equilibrium with a known amount of adsorbent. The system is held at constant temperature, pressure and ionic strength. Upon reaching steady-state, the adsorptive solution is separated from the adsorbent via centrifugation and filtration. The equilibrium concentration is then analysed to determine the degree of adsorption by using the following mass balance equation (Equation 2.12),

$$(C_0V_0) - (C_fV_f) / m = \mathrm{q} \qquad (2.12)$$

Where q is the amount of adsorption (adsorbate per unit mass of adsorbent) in mmol kg^{-1}, C_0 and C_f are the initial and final adsorptive concentrations, respectively, in mmol L^{-1}, V_0 and V_f are the initial and final adsorptive volumes, respectively, in litres, and m is the mass of adsorbent in kilograms. In this dissertation, pH envelopes are plotted with *pH* on the *x*-axis and *q* on the *y* axis.

2.7.3. Adsorption Isotherms

Adsorption isotherm illustrates the relation between the equilibrium concentration of the adsorptive and the quantity of adsorbate on the surface. The adsorption isotherm is constructed from the results of adsorption experiments. Adsorption experiments are conducted by bringing an adsorptive solution of a known concentration and volume with a known amount of adsorbent to equilibrium under constant temperature and pressure. The time that it takes for the adsorption to reach steady state is dependent on the system. The pH and ionic strength are also controlled in adsorption isotherm experiments. After equilibrium is reached, the adsorptive solution is separated from the adsorbent via centrifugation and filtration. The equilibrium

concentration is then analysed to determine the degree of adsorption by using the same mass balance equation (Equation 2.12) as for the pH envelope.

The four general types of isotherms are shown in Figure 2.8. The L-shaped or Langmuir isotherm has a decreasing slope as concentration increases, suggesting the adsorbent has a high affinity for the adsorptive at low concentration, but as the concentration increase, the affinity of the adsorptive will decrease because empty adsorbent sites are preoccupied. The S-type isotherm typically has a slope that initially increases with adsorptive concentration, but eventually decreases and becomes zero when all empty adsorbent sites are filled. The S-type isotherm is indicative of a surface with low affinity for the adsorptive under low concentrations, but adsorptivity increases with concentration. The H-type or high affinity isotherm is characteristic of a strong adsorbate-adsorptive interaction often seen in inner-sphere complexes. The C-type isotherm represents a partitioning mechanism whereby adsorptive ions or molecules are distributed or partitioned between the interfacial phase and the bulk solution phase without any specific bonding between the adsorbent and adsorbate.

2.7.4. Spectroscopy

2.7.4.1Raman Spectroscopy

Infrared (IR) and Raman spectroscopy are complementary vibrational spectroscopic techniques that provide information on molecular structure. Each functional group or structural characteristic of a molecule has a unique vibrational frequency that can be used to determine what functional groups are in a sample. A unique molecular "fingerprint" can then be established when the vibrational frequency from all the different functional groups are taken together. While IR spectroscopy detects vibrations during which the electrical dipole moment changes, Raman spectroscopy is based on the detection of vibrations during which the electrical polarisability changes (Nakamoto, 1997).

Raman spectroscopy is ideally suited for the derivation of structural information about ions in solution. Early work done by Hibben (1939) and Edwards et al. (1954) used this technique to study boric acid-borate equilibrium. Due to the relatively low concentrations involved, and the insensitivity of the instruments, polyborate species

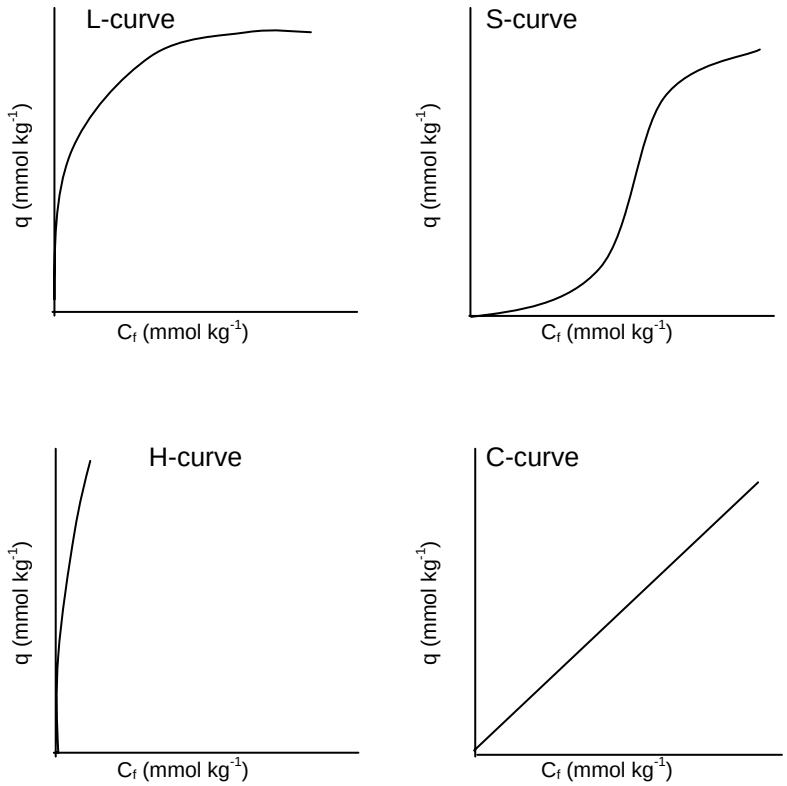

Figure 2.8 The four general categories of adsorption isotherms. Modified from Sparks (2003).

were not studied. Maya (1976) was the first to confirm the presence of polyborate ions using Raman spectroscopy and established their identity by comparison with the spectra of reference solids. Work done by Alvarez and Sparks (1985) provided the first laser Raman spectroscopic evidence of aqueous silicate anion solutions at low concentration, containing polymeric and/or other polyanionic complexes. They propose that this phenomenon may be broadened to other tetrahedrons, such as borate.

A summary of spectroscopic studies of B interactions with soil components is compiled in Table 2.3.

2.7.4.2 XAS spectroscopy

X-ray absorption spectroscopy (XAS) is a widely-used synchrotron technique applicable to answer a wide range of environmental and agricultural questions. It is an

Table 2.3 Summary of spectroscopic studies of B interaction with soil components.

Oxyanion	pH	Sorbents	Sorption Mechanism	Molecular Technique	Reference
trigonal $B(OH)_3$ and tetrahedral $B(OH)_4^-$	7-8	Am-$Al(OH)_3$	Specific adsorption	KBr pellets – transmission mode FTIR	(Beyrouty et al., 1984)
trigonal $B(OH)_3$ and tetrahedral $B(OH)_4^-$	7,11	Am-$Fe(OH)_3$	Inner-sphere	ATR-FTIR DRIFT-FTIR	(Su and Suarez, 1995)
trigonal $B(OH)_3$ and tetrahedral $B(OH)_4^-$	7,11	Am-$Al(OH)_3$	Inner-sphere	ATR-FTIR DRIFT-FTIR	(Su and Suarez, 1995)
trigonal $B(OH)_3$ and tetrahedral $B(OH)_4^-$	8	Allophane	Inner-sphere and outer-sphere	Diffuse reflectance FTIR (DRIFT)	(Su and Suarez, 1997)
trigonal $B(OH)_3$ and tetrahedral $B(OH)_4^-$	6.5-11.5	Hydrous ferric oxide	Inner-sphere and outer-sphere	ATR-FTIR	(Peak et al., 2002)

in situ spectroscopic technique that yields electronic and structural information on the element of interest. XAS has been applied to soil chemistry research because it is capable of examining samples under their natural soil conditions without destroying or altering the sample (Fendorf et al., 1994). For most environmental samples, the XAS spectra are interpreted by comparing a variety of model or reference compounds with known chemical structures against the sample; *ab initio* calculations may also be used to aid the interpretation.

X-ray absorption occurs when a core-level electron absorbs an incident X-ray with energy equal to its binding energy and is ejected from the atom as a photoelectron (Koningsberger and Prins, 1988). Since every atom has a different binding energy at every core-level, x-ray absorption edge becomes a specific character to the element of interest. Subsequent to an adsorption event, the atom is in an excited state with a core hole created by the rise of a photoelectron. The excited state will be de-excited either through 1) emitting an X-ray fluorescence photon to fill the core hole or 2) fill the core hole with an electron from a higher level and a second electron is emitted into the continuum (Stohr, 1992). The second process, termed the Auger effect, dominates in the

soft X-ray regime, whereas the first process, X-ray fluorescence is known to occur at higher energy (>2000 eV) (Stohr, 1992).

An XAS experiment, which results in a spectrum, is divided into two regions: X-ray Absorption Near Edge Structure (XANES), which includes the first 50-100 eV after the absorption edge and the Extended X-ray Absorption Fine Structure (EXAFS), which can detect up to 1000 or more eV beyond the absorption edge (Stohr, 1992).

The XANES region is extremely sensitive to the local structure and electronic environment of the element under investigation. Each chemical species can be thought of as having their own unique characteristics and the spectrum of a mixture of two or more chemical species of an element will quantitatively reflect the amount of each species in the sample being measured (Fleet and Liu, 2001). Therefore, it is possible to quantitatively determine the different chemical forms present in the sample using XANES spectroscopy. This technique is best suited for chemical components whose spectra differ substantially, whereas it is harder to distinguish or quantify spectra that are similar (Prange and Modrow, 2002) .

The assignment of features in B *K*-edge spectra of various boron-oxygen compounds and minerals has been developed (Vaughan and Tossell, 1973; Preston et al., 1976; Hallmeier et al., 1981; Ishiguro et al., 1982; Schwarz et al., 1983; Tossell, 1986; Brydson et al., 1988; Garvie et al., 1995). The edge features of XANES spectra are due to transition of the core electron to one or more unoccupied orbitals that are generally antibonding in character. The XANES of trigonal $B(OH)_3$ are characterized by the shape peak 'a' and a diffused band 'c', as in the spectrum of vitreous B_2O_3 (Figure 2.9). Peak 'a' is assigned to the transition of B 1s electrons to the unoccupied B $2p_z$ orbital, although this orbital does have significant antibonding character (π^*), the B $2p_z$ orbital is essentially non-bonding (Fleet and Muthupari, 2000). The band 'c' is assigned to transition of B 1s electrons to the unoccupied B-O sigma antibonding (σ^*) orbital, which is at a higher (~10 eV) energy than the B $2p_z$ orbital. The XANES spectra of tetrahedrally coordinated B are characterized by peak 'b' and the diffused band 'c', like in BPO_4 (Figure 2.9). Peak 'b' is assigned to transition of B 1s electrons to unoccupied sigma antibonding (σ^*) state of BO_4 (Fleet and Muthupari, 2000).

Total electron yield (TEY) and fluorescence yield (FY) are two conventional methods for measuring absorption spectra of solid samples. The TEY and FY modes measure the total number of electrons and fluorescence photons per incident photon emitted from the sample as a function of photon energy, respectively (Fleet and Muthupari, 2000). The main difference between the two modes is the sampling depth.

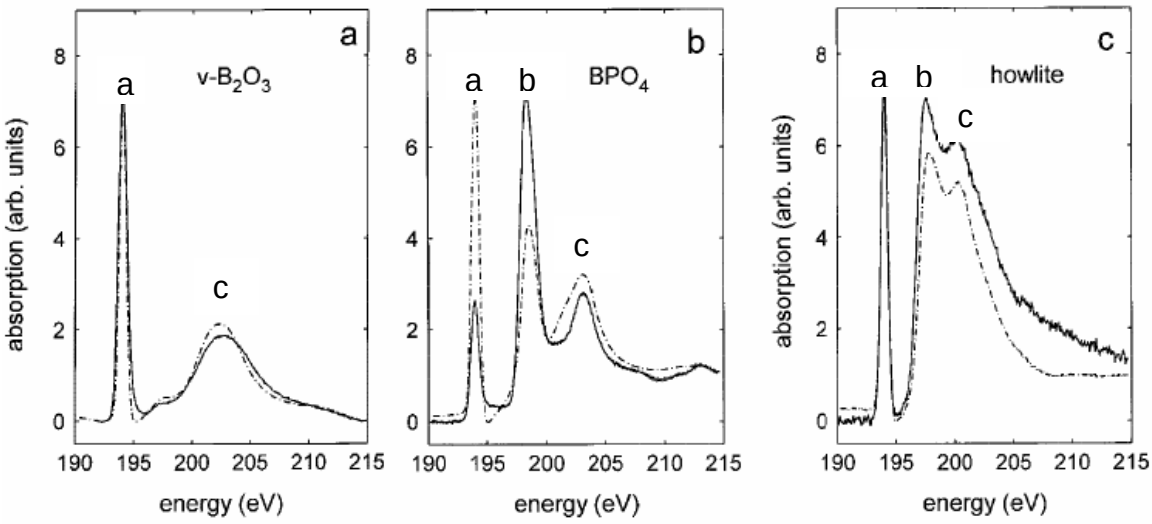

Figure 2.9 B *K*-edge XANES spectra collected in FY (solid line) and TEY (broken line) modes of (a) v-B_2O_3 with 100% trigonal $B(OH)_3$; (b) with 100% tetrahedral $B(OH)_4^-$ and (c) howlite with 80% tetrahedral $B(OH)_4^-$. Spectra have been normalized to constant height of peak 'a'. Modified from Fleet and Muthupari, (2000).

The TEY mode probes a depth of ~60 Å below the surface, making it a surface technique. The FY mode is considered as a bulk technique as a fluorescence photon at the B *K*-edge energy range (~200 eV) can achieve a maximum sampling depth of ~1100 Å for FY measurement (Kasrai et al., 1998; Fleet and Muthupari, 2000; Fleet and Liu, 2001). Differences between the TEY and FY spectra can also be attributed to surface reactions with H_2O. For example, in Figure 2.9, BPO_4 has a high amount of trigonal $B(OH)_3$ on the surface (TEY) compared to the bulk sample (FY), which could mean either the surface and the bulk sample are dramatically different from one another, or the surface has reacted with H_2O in the atmosphere to convert tetrahedral $B(OH)_4^-$ to trigonal $B(OH)_3$.

2.8. Objectives

Numerous studies have examined sorption reactions of oxyanions with soil components. Most focused on the partitioning of ions at interfaces between the solid and the aqueous phase. Interfacial processes such as adsorption at mineral-aqueous interfaces often dictate the reactivity of ions in the environment (Stumm, 1992); the knowledge of structural coordination of ions at a molecular level will enhance the understanding of these interfacial processes.

Sorption processes at mineral-aqueous interfaces are complex. Previous studies on boric acid interaction with soil minerals and organic matter were unable to provide extensive details on the reactions of B in the soil environment. However, many studies have suggested the use of vibrational molecular-scale spectroscopic studies to examine such complicated systems. Raman spectroscopy is a versatile technique that is under-utilized in the field of soil chemistry and well suited to examining systems that might be problematic for FTIR.

The fate and mobility of boric acid in the environment is directly affected by the adsorption of boric acid on soil surfaces. Boron has been found to adsorb as both outer-sphere and inner-sphere complexes on minerals commonly present in soil. The justification for this project is to provide an unambiguous evidence on the coordination of boric acid adsorption to am-$Al(OH)_3$, as well as to elucidate the effect of HA coating on adsorption of boric acid on am-$Al(OH)_3$ and hence to fill some of the gaps in current knowledge on boric acid adsorption.

The overall objective for this thesis was to investigate the effects of HA coating and dissolved CO_2 on the sorption of boric acid onto am-$Al(OH)_3$. The experimental approach for the present study was to combine macroscopic adsorption experiments with molecular-scale spectroscopic techniques to investigate boric acid reactions in the presence or absence of natural surface constituents such as humic acid and carbonate. This study represents the first use of B *K*-edge XANES spectroscopy to study boric acid adsorption on mineral surfaces.

My hypotheses are that inner- and outer-sphere complexation will occur simultaneously on mineral and humic surfaces with boric acid. The inner-sphere surface complexes (trigonal $B(OH)_3$ versus tetrahedral $B(OH)_4^-$) formed will differ from the type

of B speciation found in the solution. Reaction variables such as pH, ionic strength and concentration will dominate the type of surface complexes formed. Furthermore, the dissolved CO_2 and HA coating may impact the boric acid sorption either by reducing the availability of sorption site for boric acid or HA could enhance the dissolution of aluminum and lead to a larger availability of O-containing functional groups for boric acid adsorption.

3. ADSORPTION OF BORIC ACID ON PURE AND HUMIC ACID COATED AM-$Al(OH)_3$: A RAMAN SPECTROSCOPIC STUDY

3.1. Introduction

Much research has been devoted to studying the sorption reactions of oxyanions with soil components. Most of the research focused on the partitioning of ions at interfaces between the solid and the aqueous phase because interfacial processes such as adsorption often dictate the reactivity of ions in the environment (Stumm, 1992). There is a lack of knowledge on the structural coordination of ions at the interfaces on a molecular level; insight on structural coordination will enhance the understanding of these interfacial processes.

Sorption processes at mineral–aqueous interfaces are often complex. Previous studies on boric acid interaction with soil minerals and organic matter were unable to provide extensive details on the coordination of boric acid in the soil environment (Elrashidi and O'Connor, 1982; Gu and Lowe, 1990; Marzadori et al., 1991; Goldberg, 1997). Many studies have successfully applied molecular–scale spectroscopic studies to examine such complicated systems (Peak et al., 1999; Peak et al., 2002; Liu et al., 2003; Yamauchi and Doi, 2003).

Infrared (IR) and Raman spectroscopy are complementary vibrational techniques that can provide information on the molecular structure. Each functional group or structural characteristic of a molecule has a unique vibrational frequency that can be used to determine what functional groups are in a sample. A unique molecular "fingerprint" can then be established when the vibrational frequency from all the different functional groups are taken together. While IR spectroscopy detects vibrations during which the electrical dipole moment changes, Raman spectroscopy is based on the detection of vibrations during which the electrical polarisability changes (Nakamoto, 1997). For boric acid adsorption, vibrational spectroscopic techniques are most suitable due to the intensity and energy position of B–O vibrations (Nakamoto, 1997).

Raman spectroscopy has been widely used in the investigation of borate glass structure (Iliescu et al., 1995; Maniu et al., 2002; Yano et al., 2003; Baia et al., 2005). It is a useful method as some of the most characteristic bands for borate have been successfully identified with a vibration origin. Another advantageous feature of Raman spectroscopy is its ability to record measurements at high temperature and/or pressure (Maniu et al., 2002; Yano et al., 2003). The single drawback to Raman spectroscopy is its difficulties with quantitative treatment of spectra and their correlations with the amount of structural units, although Yano et al. (2003) did found correlation between the band intensities of BO_3 with the amount of structural units determined by ^{11}B-NMR spectroscopy.

Raman spectroscopy is also ideally suited for the derivation of structural information on borate ions in solution. Early work done by Hibben (1939) and later followed by Edwards et al. (1954) have used this technique in the past to study boric acid-borate equilibrium. Due to the relatively low concentrations involved, and the insensitivity of the instruments, polyborate species were not studied till later. Maya (1976) was the first to confirm the presence of polyborate ions using Raman spectroscopy and established their identity by comparison with the spectra of reference solids. Maeda et al. (1979) have also recorded the Raman spectra of boric acid in aqueous solutions over a wide range of pH. Recently, Liu et al. (2004) concluded in their Raman spectroscopy study of supersaturated aqueous solution of $MgO{\cdot}B_2O_3$-32%$MgCl_2$-H_2O that Raman intensities of polyborate anions vary with the change of pH. Aside from using Raman spectroscopy to study aqueous borate ions, Yamauchi and Doi (2003) also studied the distribution of B species in Japanese cedar treated with aqueous boric acid using Raman spectroscopy. They found $B(OH)_3$ to be the dominant species in wood as the bands of BO_3 group were the only bands observed (Yamauchi and Doi, 2003).

The overall goal for this study is to examine the coordination of adsorbed boric acid at am-$Al(OH)_3$ and HA coated am-$Al(OH)_3$ surfaces. The experimental approach for this research is to combine macroscopic adsorption experiments with *in situ* spectroscopic techniques to gain a better understanding of how boric acid will react under natural conditions. The objective of this experiment is to utilize Fourier transform

(FT) Raman spectroscopy to study the coordination of adsorbed boric acid on the surfaces of am-$Al(OH)_3$ and HA coated am-$Al(OH)_3$ mineral.

3.2. Material and Methods

3.2.1. Am-$Al(OH)_3$ Mineral synthesis

The predominant $Al(OH)_3$ phases in soil are the amorphous species, which are characterized by having large surface areas and greater reactivity towards anion adsorption than their crystalline counterparts (Bohn et al., 1979). Surface area is a physical property of adsorbents that is indicative of its potential reactivity. The present study has chosen to use synthetic am-$Al(OH)_3$ instead of am-$Al(OH)_3$ extracted from soils because of the superior reactivity and relative simplicity of synthesis of the former.

Various synthesis methods of am-$Al(OH)_3$ minerals have been published (Sims and Bingham, 1968; McPhail et al., 1972; Goldberg et al., 2001), and the surface areas of these amorphous minerals differ depending on the method employed. Goldberg et al. (2001) attributes the differences in surface area of am-$Al(OH)_3$ to the differences in preparation methods, especially the concentration of starting reagents. By keeping the concentrations of starting reagents ($AlCl_3$ and NaOH) under one molar and maintaining the Al : OH molar ratio at a value of 0.375, Goldberg et al. (2001) were not only able to attain a relatively high surface area mineral but the surface area remained reasonably constant with over six months of aging.

In the present study, am-$Al(OH)_3$ minerals were synthesized using four different concentrations of starting reagents (Table 3.1). In all cases, the $AlCl_3$: NaOH molar ratio were 0.375. The gel products were freeze–dried using a Virtis 25EL freeze–drier (New York, USA). The synthesized am-$Al(OH)_3$ was characterized by means of X–ray diffraction (XRD) on a Rigaku Rotaflex 200SU (Tokyo, Japan). Specific surface areas of all adsorbents were determined using both single and multipoint Brunauer–Emmett–Teller (BET) N_2 adsorption and desorption isotherms acquired with a Quantachrome Autosorb 1 Gas Sorption System (Florida, USA).

Table 3.1 Starting reagents for synthesis of freeze-dried Al oxides. †

Surface area‡	[$AlCl_3$]	[NaOH]	Supernatant solution pH	Reference
m^2g^{-1}	———— M ————			
13.05±0.64	1.5	4.0	4.30	Sims and Bingham (1968)
74.7±2.26	0.685	1.825	4.37	Goldberg et al. (2001)
140±19.8	0.408	1.088	4.51	Goldberg et al. (2001)
239±15.3	0.13	0.35	4.78	McPhail et al. (1972)
263.3 ± 5.9	0.375	1.00	4.60	This study

† $AlCl_3$/NaOH molar ratio is constant at 0.375.
‡ Single-point Brunauer-Emmett-Teller N_2.

3.2.1.1 Preparation of am-Al(OH)$_3$

Am-Al(OH)$_3$ was synthesized according to the method of Sims and Bingham (1968), modified as follows. A total of 250 mL of 1.0 M NaOH was added at a rate of 50 mL min^{-1} to a stirred solution of 250 mL of 0.375 M $AlCl_3$ inside an anaerobic chamber. The pH at the end of titration was 4.6. The mixture was shaken for 5 min and then centrifuged at 4000g for 30 min. Supernatants were discarded and gel–like precipitates were transferred to Spectra/Por® 8000 MWCO dialysis tubing for dialysis, (California, USA) until the dialysis filtrate tested negative for chloride (~ 24 hours).

3.2.1.2 Purification of humic acid

Humic acid sodium salt (Aldrich, USA) was purified following the procedure in Lemarchand et al. (2005), modified as follows. After the alkalization and acidification steps, the precipitated HAs were then washed three times with 0.1 M HCl and centrifuged again at 4000g for 30 min. The HA was then dialyzed (Spectra/Por® 8000 MWCO, California, USA) until chloride-free (~24 hours). The final HA was freeze–dried prior to use.

3.2.1.3 Preparation of 5% w/w HA coated am-Al(OH)$_3$

Humic acid coated am-Al(OH)$_3$ samples containing 5% w/w of HA were prepared by adding 0.0527 g of purified HA to 20 mL of $N_{2(gas)}$ purged (CO_2 free) 0.1 M NaOH solution. This HA solution was then adjusted to pH 7.5 via the addition of 1.0 M

NaOH. The completely dissolved HA solution was then mixed with 1.0 g of pure am-$Al(OH)_3$ and shaken for 24 hours.

3.2.2. Point of zero charge (PZC)

The Zetasizer Nano ZS and MPT-2 Autotitrator (Malvern, UK) were used to determine the PZC through the measurement of zeta potential as a function of pH. Am-$Al(OH)_3$ or HA coated am-$Al(OH)_3$ at a solid density of 1.0 g L^{-1} were first added to the folded capillary zeta potential cell. The zeta potential measurements were made in 3 replicates from pH 5 to 10. The pH of the samples was adjusted via the addition of 1.0 M HCl or 1.0 M NaOH, made with the automated MPT-2 Autotitrator. The PZC were plotted with pH on the x-axis and zeta potential on the y-axis.

3.2.3. Adsorption envelopes

Batch boric acid adsorption envelope experiments were conducted on am-$Al(OH)_3$ and 5% w/w HA coated am-$Al(OH)_3$ at 25 °C under anaerobic conditions. These experiments were conducted in 0.1 M NaCl as a function of pH. Am-$Al(OH)_3$ (0.04 g) or 5% w/w HA coated am-$Al(OH)_3$ (0.04 g) were added to reaction vessels with 40 mL of 0.1 M NaCl containing $[B(OH)_3]_{init}$ at either 0.3 mmol L^{-1} or 1.5 mmol L^{-1}. The suspensions were adjusted to their desired pH with 1.0 M HCl or 1.0 M NaOH inside an anaerobic chamber. The total amount of base added resulted in less than a 2.5% change in ionic strength. The pH of the system was measured after 24 hours of equilibration. The supernatant was separated from the mineral by centrifugation at 4000g for 30 min and then filtered through 0.25-µm membrane (Millipore). Boron concentration was determined colorimetrically using the Azomethine–H method described by Bingham (1982). The amount of B adsorbed was calculated by subtracting the total boric acid equilibrium concentration from the initial boric acid concentration. The B loading rate is calculated based on mineral weight, determined gravimetrically.

3.2.4. Adsorption isotherms

Batch experiments were conducted for boric acid adsorption on am-$Al(OH)_3$ and 5% w/w HA coated am-$Al(OH)_3$ at 25 °C in either an anaerobic chamber or under atmospheric conditions to determine the amount of adsorbed B, as a function of initial

boric acid concentration in 0.1 M NaCl at pH 5.9 or 9.2. Am-$Al(OH)_3$ (0.04 g) and 5% w/w HA coated am-$Al(OH)_3$ (0.04 g) were added to the reaction vessel with 40 mL of 0.1 M NaCl containing a known concentration of boric acid. The suspensions were adjusted to their desired pH with 1.0 M HCl or 1.0 M NaOH inside an anaerobic chamber or under atmospheric conditions. For atmospheric experiments, the amount of dissolved CO_2 was controlled by exposure to the atmosphere during the pH adjustment period as well as the presence of atmospheric levels of CO_2 in the headspace (10 mL) during the equilibration period. The total amount of base added (100 μL max) resulted in less than a 2.5% change in ionic strength. The pH of the systems was measured after 24 hours of equilibration. The supernatant was separated from the mineral by centrifugation at 4000 g for 30 min and then filtered through 0.25-μm filters (Millipore). Boron concentration and loading rates were determined colorimetrically using the Azomethine–H method described in the previous section.

3.2.5. FT–Raman

Raman spectra of all the solids, liquids and gel pastes were recorded with a Bruker Equinox FRA 106 FT–Raman spectrometer (Ettlingen, Germany) equipped a XPM detector and a CaF_2 beamsplitter. The excitation source for the Raman was an Nd: YAG laser (1060 nm) in the 180° back–scattering configuration. The incident laser beam was approximately 0.1 mm in diameter. The incident laser power for solid and liquid/gel paste samples was 60 mW and 500 mW, respectively. The different laser powers were selected to generate an interferogram with a strong center burst from the sample, while preventing irreversible thermal damage. All the FT–Raman spectra were recorded at ambient temperature from 3500 – -2000 cm^{-1} with a resolution of 2 cm^{-1}. When preparing samples for FT–Raman spectroscopy, care was taken to ensure that as much of the sample as possible was positioned in the foci of the laser beam. Solid powdered samples and gel pastes were packed into small aluminum disks, while quartz cuvettes were used for liquid samples. Bands of the quartz were removed by performing a spectral subtraction.

Data reduction and analysis were performed using Opus version 4.2 (Ettlingen, Germany). First, the individual spectra were averaged. Second, the spectra were cut to

the desirable range, and spectrum subtracted by the appropriate background spectra. Finally, the spectra were baseline corrected using the Rubberband Correction with 64 baseline points and normalized to scale.

3.3. Results and Discussions

The surface area for am-$Al(OH)_3$ was 263.3 ± 5.9 m^2g^{-1}. However, with oven drying samples such as amorphous metal oxide and humic substances can change their structure and strongly affect the adsorption of $N_{2(gas)}$. For this reason, it is difficult to conclusively monitor changes in specific surface area upon humic acid coating of our samples. The PZC values of am-$Al(OH)_3$ and 5% w/w HA coated am-$Al(OH)_3$ were 8.45 and 7.86, respectively; these values are in agreement with reported values for similar phases (Varadachari et al., 1997). A decrease in PZC was observed in 5% w/w HA coated am-$Al(OH)_3$ compared to pure am-$Al(OH)_3$ (Figure 3.1 and 3.2), which indicates specific adsorption of HA on the mineral surface, and is consistent with previous studies (Marzadori et al., 1991; Gu et al., 1994; Pizer and Ricatto, 1994). The change in surface charge associated with HA adsorption may increase the adsorption of borate anions at pH values below the PZC of the mineral.

3.3.1. Macroscopic Studies

XRD showed that the am-$Al(OH)_3$ (Figure 3.3) remained non-crystalline throughout the adsorption experiments. Boric acid pH envelopes from the batch experiments exhibited a parabolic form (Figure 3.4), similar to previous studies on B adsorption on aluminum oxide minerals (Goldberg and Glaubig, 1985).

Boric acid adsorption on am-$Al(OH)_3$ and 5% w/w HA coated am-$Al(OH)_3$ showed an increase in adsorption from pH 4.5 – 9.0 with the adsorption maxima located at approximately pH 9.2 (the pKa of boric acid). There were only minor adsorption differences on a per mass basis between the two adsorbents at $[B(OH)_3]_{tot}$ of 0.38 mmol L^{-1}. However, there was a two fold increase in adsorption with am-$Al(OH)_3$ compared to 5% w/w HA coated am-$Al(OH)_3$ at $[B(OH)_3]_{tot}$ of 1.51 mmol L^{-1}.

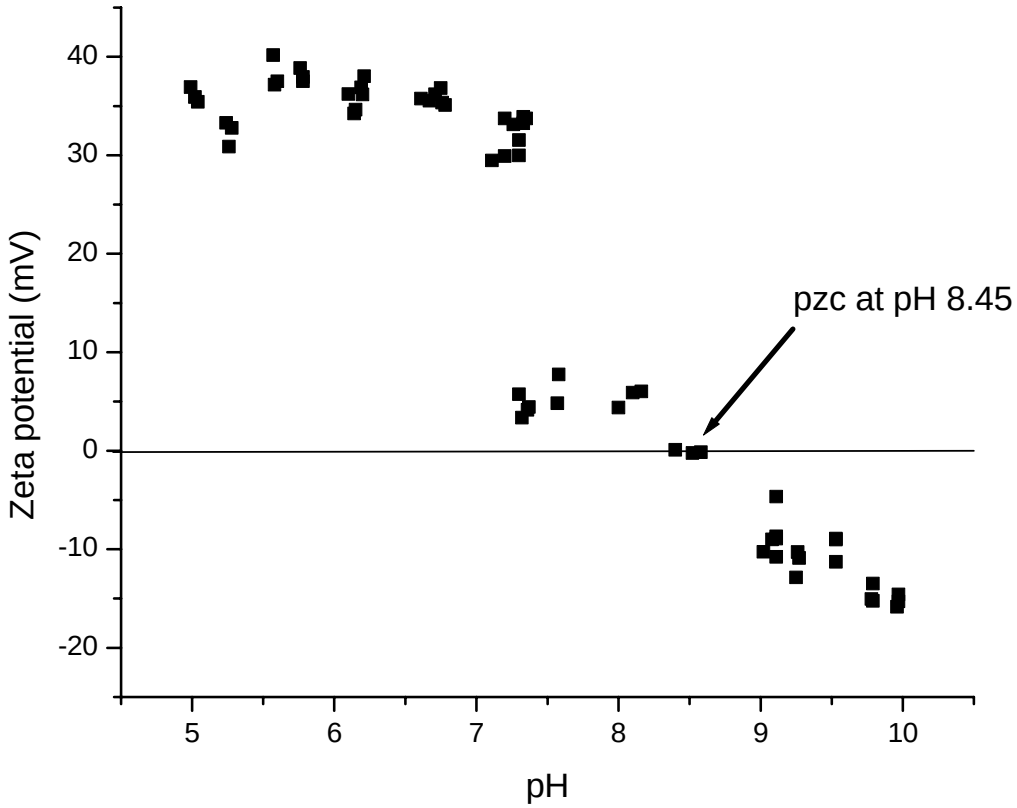

Figure 3.1 Isoelectric point of am-$Al(OH)_3$.

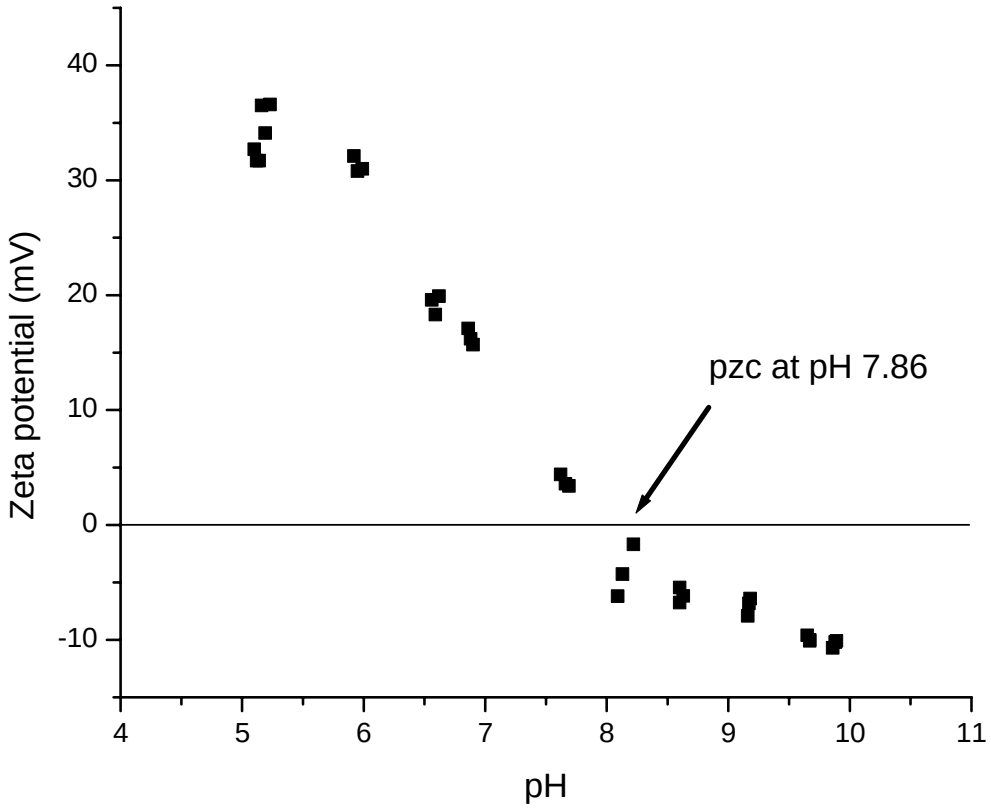

Figure 3.2 Isoelectric point of HA coated am-$Al(OH)_3$.

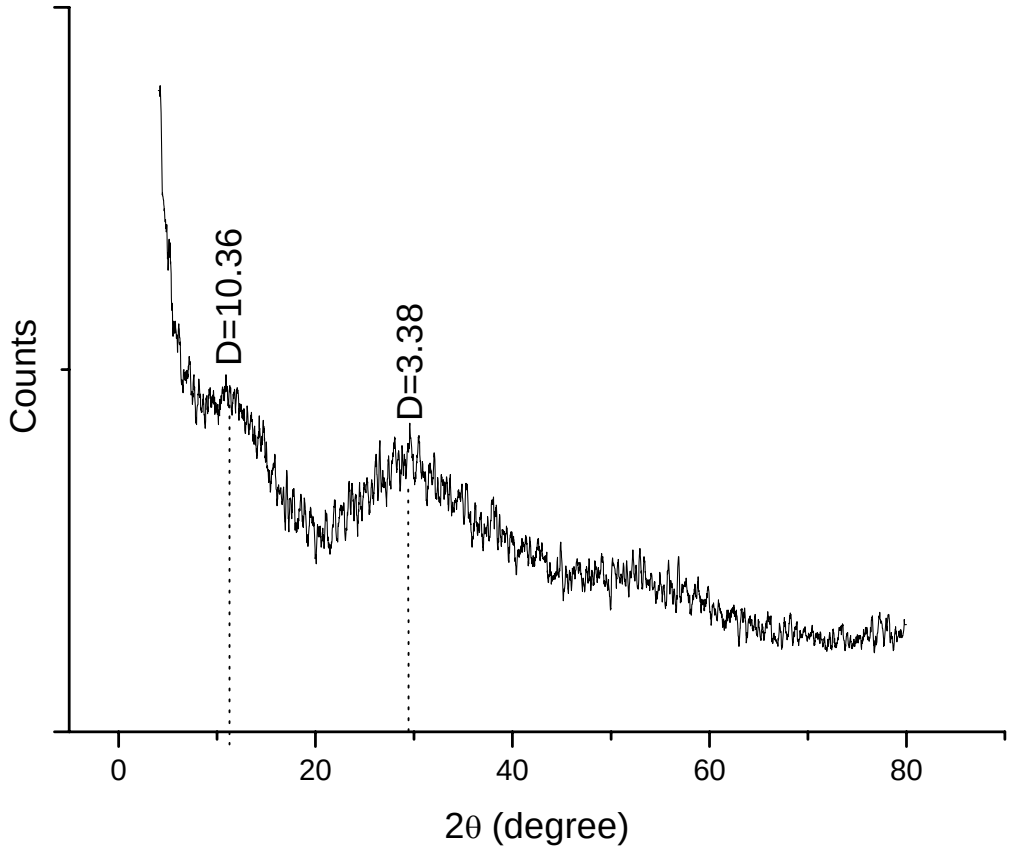

Figure 3.3 XRD of am-$Al(OH)_3$ after freeze drying. D–spacings are indicated in Å.

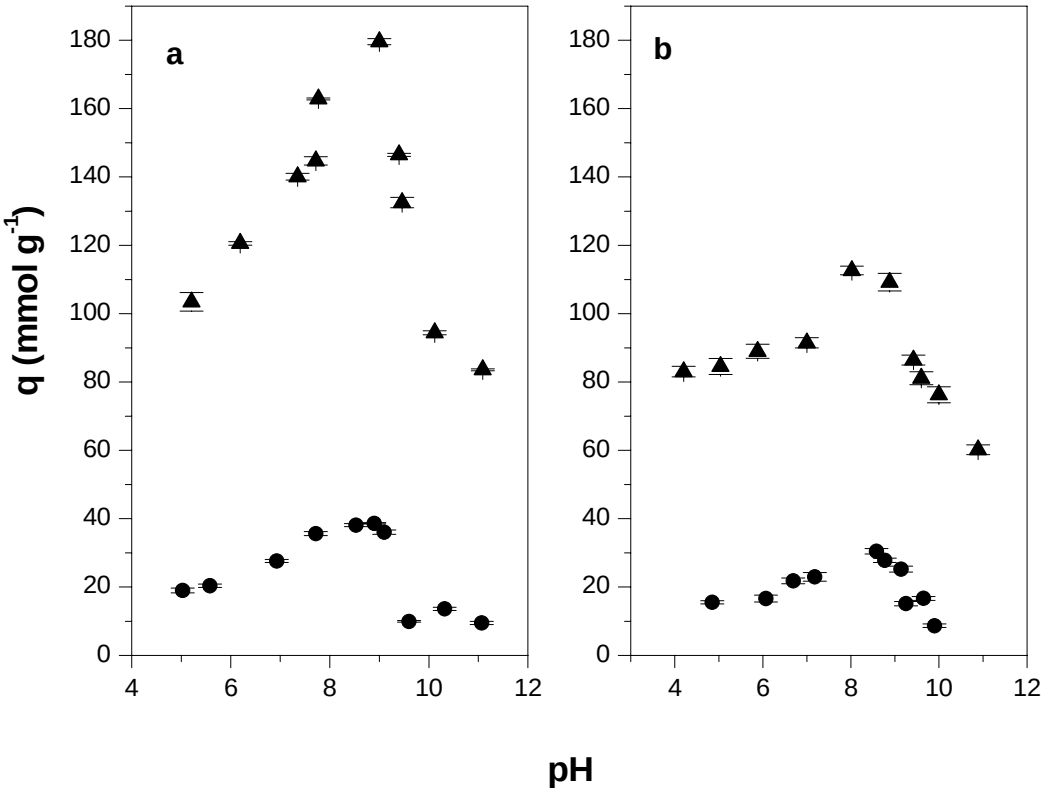

Figure 3.4 Boric acid pH envelopes from batch adsorption experiments. ▲represents $[B(OH)_3]_{init}$ = 1.51 mmol L^{-1} and ● represents $[B(OH)_3]_{init}$ = 0.38 mmol L^{-1} and a) is am-$Al(OH)_3$ and b) is 5% w/w HA coated am-$Al(OH)_3$. Error bar indicate standard deviation, maybe covered by symbols.

Boric acid adsorption isotherms exhibited an "S–shaped" curve (Figure 3.5), which is indicative of low affinity for boric acid adsorption at low boric acid solution concentrations and greater affinity for adsorption as solution concentration increases. Greater boric acid adsorption of both surfaces occurred at pH 9.2 than at pH 5.9. At both pH 5.9 and 9.2, the presence of dissolved CO_2 decreased boric acid adsorption of both pure and HA coated minerals. Despite the change in surface charge associated with HA sorption, HA coating did not affect boric acid adsorption in systems under N_2. Boric acid adsorption was most strongly affected by the combination of HA coating and the presence of dissolved CO_2. This decrease in boric acid adsorption may be a consequence of (1) carbonate and bicarbonate adsorption leading to the formation of protonated surface groups, and (2) the change in surface charge due to HA sorption.

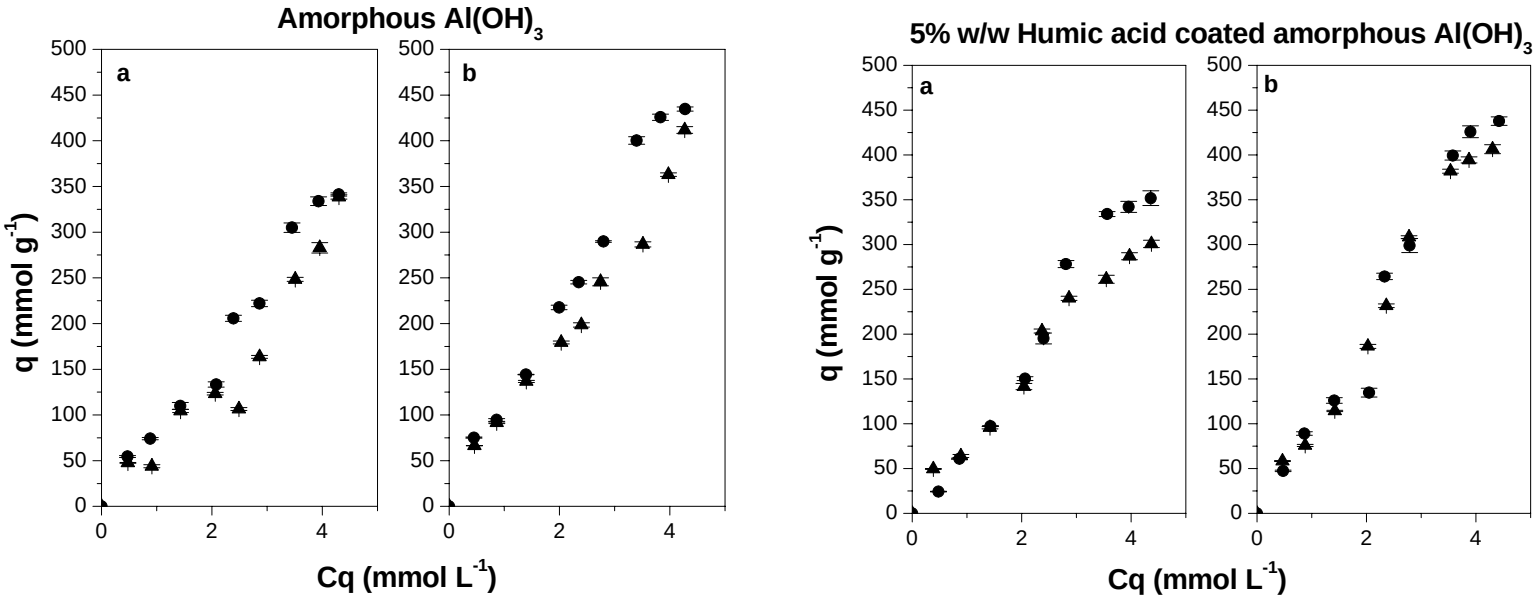

Figure 3.5 Boric acid adsorption isotherms from batch adsorption experiments. ▲represents system opened to atmosphere and ● represents system under N_2 and a) under pH 5.9 ± 0.1 and b) under pH 9.2 ± 0.03. Error bar indicate standard deviation, maybe covered by symbols.

3.3.2. FT–Raman

In order to identify Raman bands of trigonally and tetrahedrally coordinated B in mineral-aqueous interfaces, we analyzed a variety of solid, liquid and pastes samples. Table 3.2 complies all the observed frequencies of FT Raman in the 500-1500 cm^{-1} region of solid B standard compounds, boric acid solution as well as am-$Al(OH)_3$ pastes with a known amount of B adsorbed on it. Figure 3.6 is a normalized FT-Raman spectra of solid boric acid, sodium tetraborate decahydrate, aqueous 100 mmol L^{-1} boric acid solution and washed am-$Al(OH)_3$ paste with 213 mmol B kg^{-1} loading rate. A symmetrical BO_3 stretching vibration, ν_1, which is Raman active and characteristic, appears at 880cm^{-1} in the solid boric acid samples. In the aqueous and mineral paste samples the same band is observed at a slightly lower wavenumber (878cm^{-1}), indicating the presence of trigonal $B(OH)_3$. Raman lines at 499cm^{-1} (O—B—O bending, $\nu 2$) and 1167cm^{-1} (B—O—H bending, $\nu 3$) are present in the solid samples but not detectable in the aqueous and paste samples. No B species other than trigonal $B(OH)_3$ could be identified from the Raman spectra in the aqueous and mineral paste samples. Detection of Raman bands of adsorbed B on 5% w/w HA coated am-$Al(OH)_3$ is more difficult than on am-$Al(OH)_3$ due to the presence of two broad bands at 696 and 1084 cm^{-1} (Figure 3.7).

Table 3.2 Observed frequencies of FT–Raman spectra.

FT–Raman				Assignment
Solid	**Liquid**	**Am-$Al(OH)_3$**	**5% w/w HA coated am-$Al(OH)_3$**	
499 (m)		498(w)		ν_2 (O-B-O) bending
575 (s)				ν_s (B-O) in trigonal BO_3
			696 (b)	C-H bending of CH_2 and CH_3 groups
880 (sh)	877-878(w)	878-879(w)		ν_s (B-O) in trigonal BO_3
946 (w)				ν_s (B-O) in tetrahedral BO_4
			1084 (b)	C-H stretch of CH_2 and CH_3 groups
1167 (m)				ν_3 (B-O-H) bending

w = weak, m = moderate, s = strong, sh = sharp, br = broad

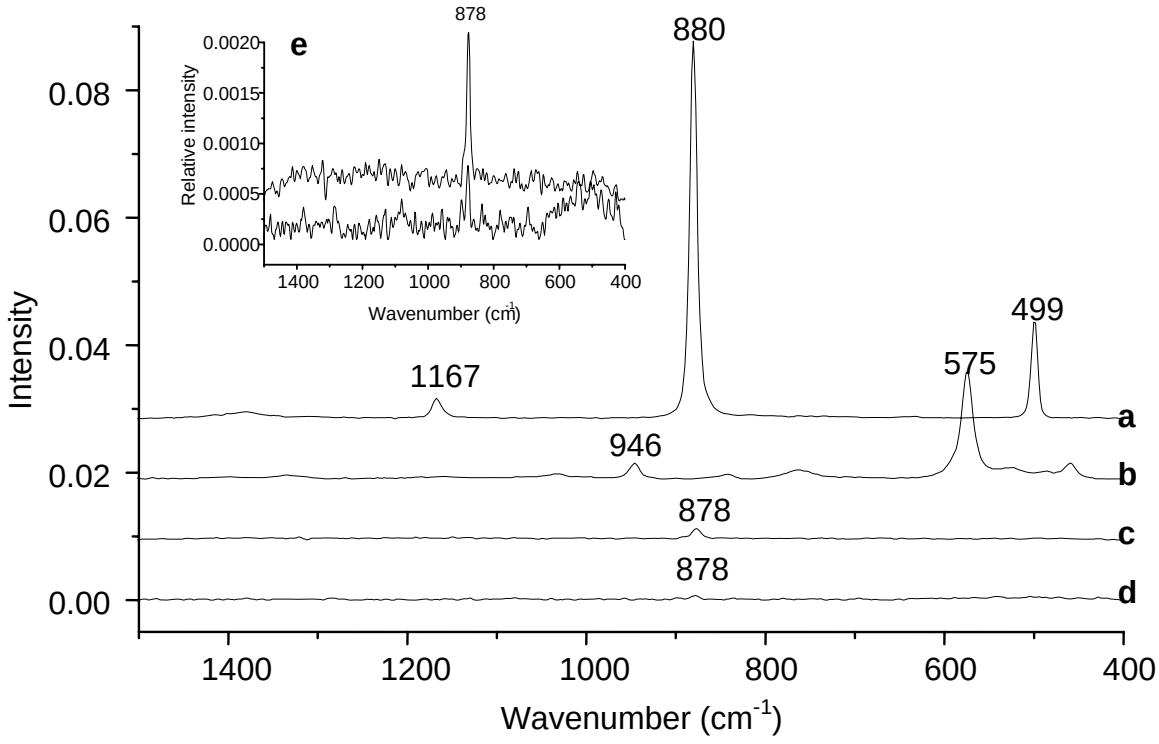

Figure 3.6 FT–Raman spectra of a, solid boric acid; b, solid sodium tetraborate decahydrate; c, aqueous 100 mmol L^{-1} boric acid; d, washed am-$Al(OH)_3$ with loading rate of 213 mmol B kg^{-1} and e, expanded view of c and d.

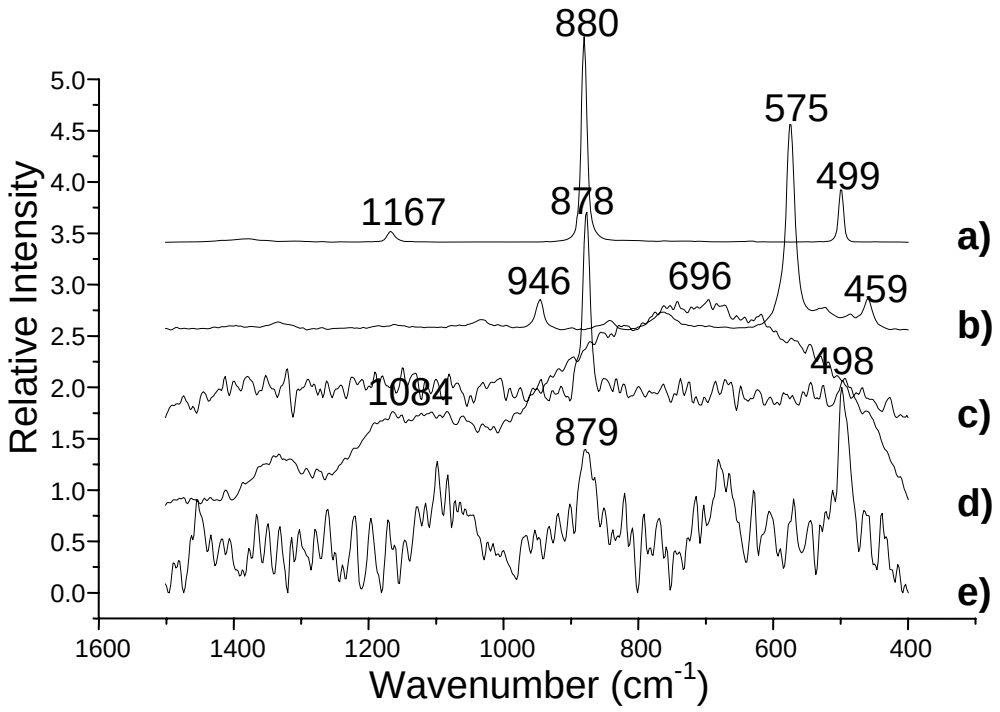

Figure 3.7 Normalized FT-Raman spectra of a) solid boric acid; b) solid sodium tetraborate decahydrate; c) aqueous 100 mmol L^{-1} boric acid; d) 5% w/w HA coated am-$Al(OH)_3$ paste with loading rate of 457.27 mmol B kg^{-1} and e) am-$Al(OH)_3$ paste with loading rate of 563.50 mmol B kg^{-1}.

3.4. Conclusions

The understanding of boric acid adsorption and coordination on soil mineral/aqueous interface is important for the assessing the bioavailability of B in the environment. Much research emphasis has been placed on the study of boric acid-organic acid (i.e. HA) complexation (Gu and Lowe, 1990; Lemarchand et al., 2005; Marzadori et al., 1991), whereas very few studies focused on the influence of HA on the dynamics of boric acid adsorption by soil minerals. The present study has investigated the influence of HA on boric acid adsorption by am-$Al(OH)_3$ mineral, both as a function of pH (4.5 – 11) and initial boric acid concentration (0 – 4.5 mmol L^{-1}).

Boric acid adsorption isotherms showed greater boric acid adsorption occurred under pH 9.2 than 5.9. HA coating had a smaller effect on boric acid adsorption at pH 5.9 compared to pH 9.2. Under the same pHs, the presence of dissolved CO_2 had a more pronounced effect on boric acid adsorption than the system under anaerobic environment. In general, the combination of HA coating on the am-$Al(OH)_3$ mineral and the presence of dissolved CO_2 had the greatest impact on boric acid adsorption. Vibrational spectroscopy may sound like an ideal technique for probing the coordination of boric acid adsorbed on mineral and HA coated mineral phases; however the experimental limitation for Raman spectroscopy is well above the point of polymerization for aqueous boric acid (~25 mmol L^{-1}). Furthermore, it is difficult to identify any B bands in 5% w/w HA coated am-$Al(OH)_3$ paste due to bands overlapping with B-O stretching modes.

Future Raman experiments conducted under low temperature might be able to provide better quality spectra.

4. COORDINATION OF BORIC ACID WITH SOIL MINERALS AND SOIL ORGANIC MATTER: A XANES STUDY

4.1. Introduction

Boron (B) is one of several essential micronutrients required by plants at low levels. Boron is thought to be important during the development of cell walls and for the structural integrity of dicotyledonous plant cell walls (Ascerbo et al., 1973). Phototoxic levels of B are often associated with arid environments where soil is naturally rich in B minerals such as colemanite, kernite, ulexite and borax (Keren and Bingham, 1985). The labile fraction of B (mostly the mononuclear species of boric acid $B(OH)_3$ and borate $B(OH)_4^-$) are available for plants to utilize, but these two species account for only 10% of total soil B content (Xu et al., 2001).

Numerous studies have examined sorption reactions of boric acid with soil components such as clay minerals and metal oxides (Goldberg and Glaubig, 1985; Goldberg and Glaubig, 1986b; Bloesch et al., 1987; Goldberg and Glaubig, 1988). Boric acid adsorption is affected by pH, ionic strength, temperature, competitive ligands, and organic matter content (Marzadori et al., 1991; Goldberg et al., 1993a; Goldberg et al., 1993c; Keren and Sparks, 1994; Yermiyahu et al., 1995; Goldberg et al., 1996). Studies by Su and Suarez (1995) and Peak et al. (2002) have used attenuated total reflectance Fourier transform infrared (ATR-FTIR) spectroscopy to investigate the coordination of adsorbed B on am-$Fe(OH)_3$. Both studies found spectroscopic evidence that both trigonal $B(OH)_3$ and tetrahedral $B(OH)_4^-$ adsorb on am-$Fe(OH)_3$ mineral surfaces via inner-sphere (ligand-exchange) and outer-sphere complexation (Su and Suarez, 1995; Peak et al., 2002). Su and Suarez (1995) also studied boric acid adsorption on am-$Al(OH)_3$ surfaces, but were not able to detect any tetrahedral $B(OH)_4^-$ complexes using ATR-FTIR spectroscopy due to the strong interference bands from Al-O vibrations.

Atmospheric CO_2 can be readily dissolved in water to form $CO_{2(aq)}$, H_2CO_3, HCO_3^- and CO_3^{2-} species. Studies that have encompassed carbonate species in adsorption experiments showed that they either decreased the sorption of oxyanions on metal oxides (Schulthess and McCarthy, 1990; Van Green et al., 1994; Duff and Amrhein, 1996) or they promoted the adsorption of oxyanions via the generation of extra protonated surface groups (Wijnja and Schulthess, 2000; Wijnja and Schulthess, 2002). The impacts of dissolved CO_2 and CO_3^{2-} species have not been specifically examined in previous B adsorption studies.

X-ray Absorption Near Edge Structure (XANES) is a molecular-scale spectroscopic technique that yields electronic and structural information on the element of interest. Each chemical species has its own unique characteristics and the spectrum of a mixture of two or more chemical species of an element will quantitatively reflect the amount of each species in the sample being measured, allowing the use of XANES spectroscopy to quantitatively determine different chemical forms present in the sample (Fleet and Liu, 2001).

Boron *K*-edge XANES spectroscopy has been used to differentiate between trigonally and tetrahedrally-coordinated B complexes in borate and borosilicate minerals (Li et al., 1996; Kasrai et al., 1998; Fleet and Muthupari, 2000; Fleet and Liu, 2001). Fleet and Liu (2001) found that B *K*-edge XANES spectra collected in total electron yield (TEY) mode, which probes to < 60 Å, were markedly different than spectra collected in fluorescence yield (FY) mode, which is a bulk structure technique.

The overall objective for this chapter was to investigate the effects of HA coating and dissolved CO_2 on the sorption of boric acid onto am-$Al(OH)_3$. The experimental approach for the present study was to use molecular-scale spectroscopic techniques to investigate boric acid reactions in the presence or absence of natural surface constituents such as humic acid and carbonate. This study represents the first use of B *K*-edge XANES spectroscopy to study boric acid adsorption on mineral surfaces.

4.2. Material and Methods

4.2.1. Mineral Synthesis and Characterization

Am-$Al(OH)_3$ was synthesized according to the method of Sims and Bingham (1968), modified as follows. A total of 250 mL of 1.0 M NaOH was added at a rate of 50 mL min^{-1} to a stirred solution of 250 mL of 0.375 M $AlCl_3$ inside an anaerobic chamber. The pH at the end of titration was 4.6. The mixture was shaken for 5 min and then centrifuged at 4000g for 30 min. Supernatants were discarded and gel–like precipitates were transferred to Spectra/Por® 8000 MWCO dialysis tubing for dialysis, (California, USA) until the dialysis filtrate tested negative for chloride (~ 24 hours).

Humic acid sodium salt (Aldrich, USA) was purified following the procedure of Lemarchand et al. (2005), modified as follows. After the alkalization and acidification steps, the precipitated HAs were then washed three times with 0.1 M HCl and centrifuged again at 4000g for 30 min. The HA was then dialyzed (Spectra/Por® 8000 MWCO, California, USA) until chloride-free (~24 hours). The final HA was freeze–dried prior to use.

Humic acid coated am-$Al(OH)_3$ samples containing 5% w/w of HA were prepared by adding 0.0527 g of purified HA to 20 mL of N_2 purged 0.1 M NaOH solution. This HA solution was then adjusted to pH 7.5 via the addition of 1.0 M NaOH. The completely dissolved HA solution was then mixed with 1.0 g of pure am-$Al(OH)_3$ and shaken for 24 hours.

4.2.2. X-ray Absorption Near Edge Structure Spectroscopy

Samples for XANES spectroscopy were made up of crystalline boric acid compounds, various borate mineral standards and B adsorption samples. Boron adsorption samples were freeze-dried powders obtained via centrifugation of equilibrated mineral-solution suspensions prepared by the method described in the previous section of 3.2.2. The mineral pastes were rinsed with 120 mL of 18.2 MΩ water following centrifugation to remove any B in the entrained solution and then freeze-dried. The freeze drying process is required to run adsorption samples at the B *K*-edge energy in solid or powder form. While we recognize that freeze drying has the potential to change surface complexes due to removal of some surface waters, it is a

much less destructive method than oven drying. Boron *K*-edge XANES spectra were recorded at the Canadian Light Source (Saskatoon, SK) on the Variable Line Spacing Planar Grating Monchromator beamline. This beamline is monochromatized by three variable line spaced gratings over the photon region of 5 to 250 eV and yields a photon resolution > 10 000 eV/delta eV in the B *K*-edge region (~193.6 eV) (Reininger et al., 2002). The vacuum at the sample is between 10^{-8} to 10^{-9} torr. A micro-channel-plate detector was used to record the FY spectrum; detailed information on the detection system is described in the literature (Kasrai et al., 1993). The TEY spectrum was obtained by measuring the sample current as the result of the photoabsorption.

All XANES spectra were obtained in the same experimental session. Data from the TEY and FY yields were collected simultaneously. Mineral samples were analyzed as fragments, while adsorption samples were lightly mixed with a mortar and pestle before mounting on carbon tape for analyses. Data reduction and analyses were performed using WinXAS version 3.1 software (Berlin, Germany). The individual spectra were first averaged, a linear baseline correction was performed between 190 and 192 eV, and finally the spectra were all normalized to an edge step of 1 from 190 to 212.2 eV. Difficulties in normalization of the sorption samples were sometimes observed in the post-edge region (between 210 and 215 eV), which do not overlap exactly. However, only quantitative analyses were made in the absorption edge region (from 193-195 eV), where normalization was done correctly and the spectra can overlie on each other. For other energies, the discussion will be limited to qualitative observations only.

4.3. Results and Discussions

4.3.1. Characteristics of the minerals

The surface area for am-$Al(OH)_3$ was 263.3 ± 5.9 m^2g^{-1}. However, drying samples such as amorphous metal oxide and humic substances can change their structure and strongly affect the adsorption of $N_{2(gas)}$. For this reason, changes in specific surface area upon humic acid coating of our samples were not monitored.

4.3.2. Boron K-edge XANES spectroscopy

4.3.2.1 Boron Reference Compounds

Polynuclear B species are not known to form at boric acid concentrations under 25 mmol L^{-1} (Cotton and Wilkinson, 1989). Even at boric acid concentrations of 100 mmol L^{-1}, less than 5% w/w polynuclear species are present (Bloesch et al., 1987). In the present study, it was assumed that the XANES spectra of boric acid adsorption samples at pH 7.0 and 9.2 were dictated predominantly by mononuclear species.

Various borate standard minerals were analyzed with B *K*-edge XANES spectroscopy to identify peaks attributed to trigonally and tetrahedrally-coordinated B (Figure 4.1). Results in this study were very similar to Fleet and Muthupari's B *K*-edge study on borate minerals (Fleet and Muthupari, 2000). Specifically, diagnostic peaks 'a' and 'c' (Figure 4.1) for trigonal $B(OH)_3$ were present in the boric acid standard and borate mineral standards known to contain trigonal $B(OH)_3$ species.

Differences seen in TEY and FY-XANES spectra (Figure 4.1) of the borate minerals (especially boric acid standard) indicates that the chemical compositions of the surface and bulk sample were different. The dissimilarities between the TEY and FY-XANES spectra can be attributed to mechanical damage and/or hydration of the mineral (Kasrai et al., 1998). Self absorption was evident in the FY-XANES spectra of the boric acid as the height of peak 'a' is dampened compared to its corresponding TEY-XANES spectra (Figure 4.1).

The height of peak 'a' from the TEY-XANES spectra of mineral standards were strongly linearly correlated to % trigonal $B(OH)_3$ ($R^2 = 0.9428$) (Figure 4.2). Peak 'b', characteristic of tetrahedrally coordinated B, was present in danburite, a mineral known to contain 100% tetrahedral $B(OH)_4^-$ and other borate minerals that contain over 50% tetrahedral $B(OH)_4^-$ proportionally (Figure 4.1).

The only dramatic difference between this study and Fleet and Muthupari's study (2000) was the TEY-XANES spectra for the 100% tetrahedral $B(OH)_4^-$ mineral. This study used danburite as the tetrahedral $B(OH)_4^-$ standard, while Fleet and Muthupari (2000) used BPO_4. The TEY and FY-XANES spectra for danburite were consistent with tetrahedrally coordinate B features, while the TEY-XANES spectra for BPO_4^- had trigonal $B(OH)_3$ features and the FY-XANES spectra had primarily tetrahedral $B(OH)_4^-$ features. The differences between the TEY and FY-XANES spectra could be the result of surface reaction (i.e. hydration) or cross-contamination.

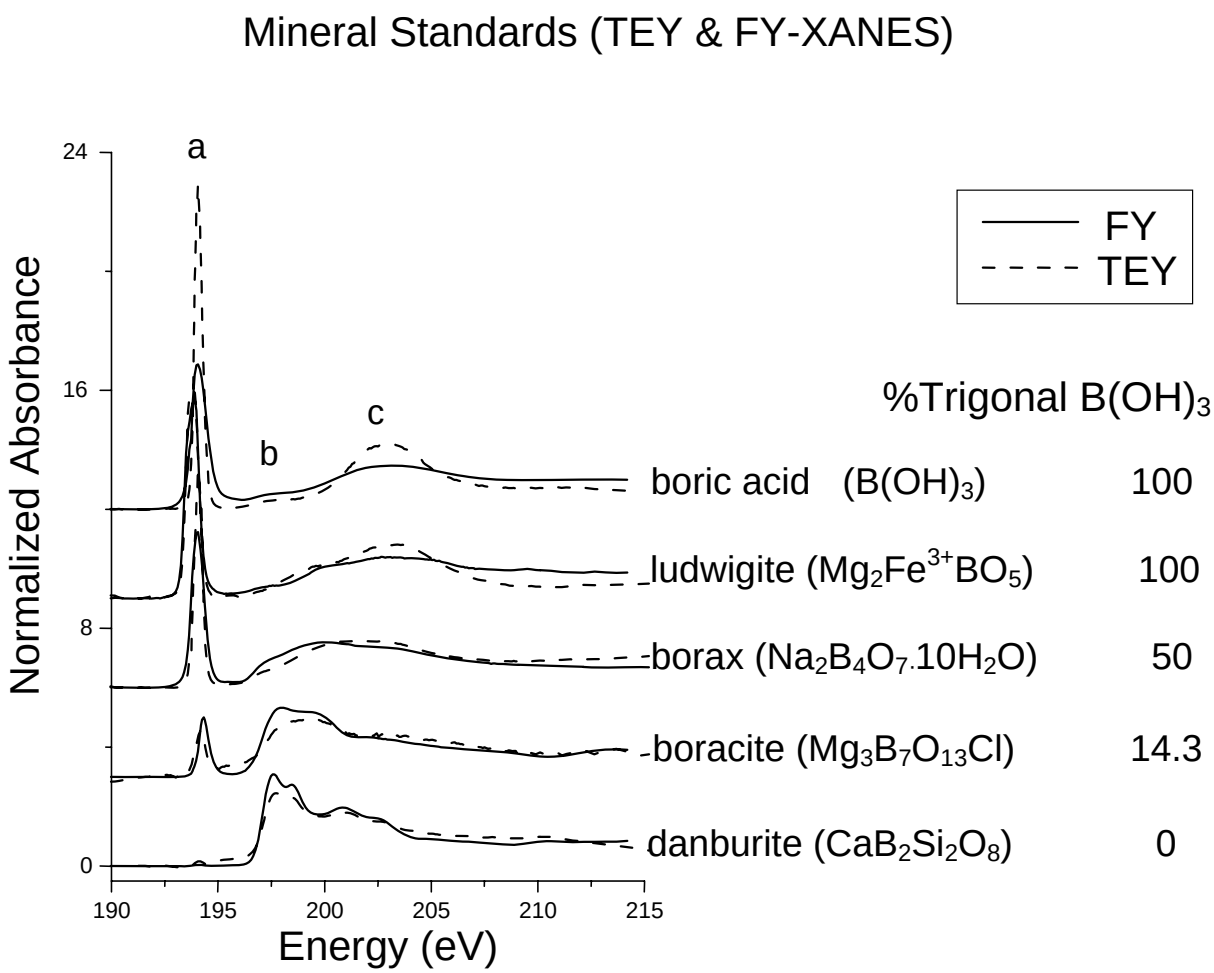

Figure 4.1. B *K*-edge XANES (X-ray absorption near-edge structure) spectra collected in FY (fluorescence yield) mode (solid line) and TEY (total electron yield) mode (dashed line) for six selected borate standards.

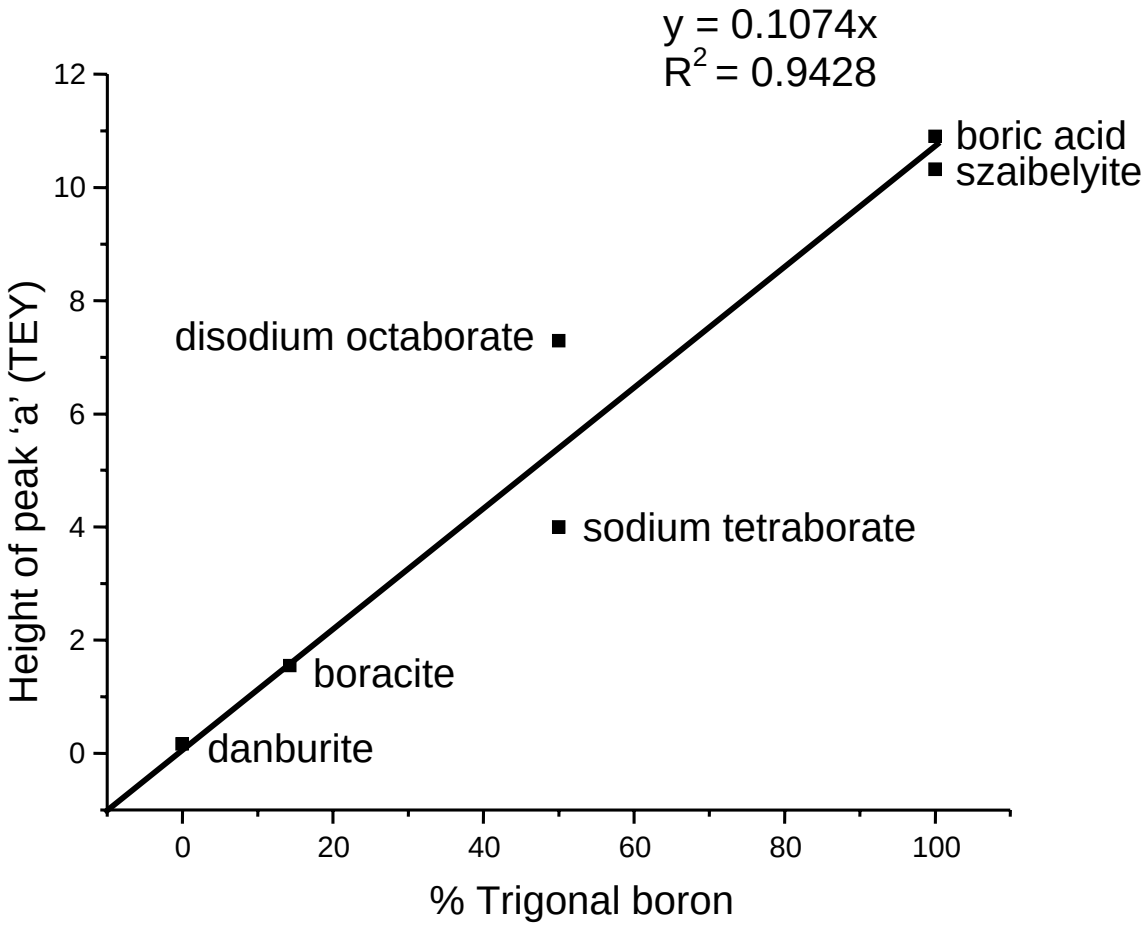

Figure 4.2 The height of peak 'a' in the TEY- XANES spectra of borate mineral standards correlated with % trigonal $B(OH)_3$.

The peak 'a' in mineral ludwigite ($Mg_2Fe^{3+}BO_5$) was shifted to a lower energy (Figure 4.1) as a result of complexation of trigonal $B(OH)_3$ with a 3d transition metal. Previous studies have also reported a downshift in energy for the white line (peak 'a') resulting from interactions between the 2p state of the binding atom and the 3p and 3d states of metal cations (Okude et al., 1999; Khare et al., 2005).

4.3.2.2 Boron Adsorption Isotherm Samples – Self Absorption Effects

The FY-XANES spectra of boric acid adsorption on am-$Al(OH)_3$ under N_2 at both pH 7.0 and 9.2 were substantially different from its corresponding TEY-XANES spectra (Figure 4.3). Surface reaction such as hydration may have contributed to the differences seen in the FY and TEY-XANES spectra. Self absorption may also have impacted samples with high B loading rate (>2000 mmol Kg^{-1}). This self absorption effect seen in the FY-XANES spectra was apparent through the reduction in the height of peak 'a' (Figure 4.3). This can clearly be observed in the increase in peak height ratio between the peak 'a' TEY: peak 'a' FY (Table 4.1) as loading rate increases. Self absorption has an effect on the quantitative analysis of the system: height of peak 'a' in TEY-XANES was strongly linearly correlated to B loading rate ($R^2 = 0.9051$) while the height of peak 'a' in FY-XANES was less closely correlated to B loading rate ($R^2 = 0.7993$).

4.3.2.3 Boron Adsorption Isotherm Samples – Effects of Dissolved CO_2 and Humic Acid

Figure 4.4(A) and (B) show TEY-XANES spectra for the boric acid adsorption on am-$Al(OH)_3$ and 5% w/w HA am-$Al(OH)_3$ under both anaerobic and atmospheric conditions at pH 7.0 and 9.2, respectively. Figure 4.5(A) and (B) show the corresponding FY-XANES spectra for above-mentioned samples at pH 7.0 and 9.2, respectively.

Generally, the shape and peak positions for the samples are similar, and the major difference between the TEY and FY-XANES data is the dampening of the peak 'a' intensity that can be attributed to self absorption effects.

Data for the adsorption samples, including B loading rate, position and height of peak 'a', are listed in Table 4.2. The height of peak 'a' from the TEY-XANES spectra

Table 4.1 Boric acid adsorption isotherm freeze dried gel samples analyzed by B *K*-edge XANES (X-ray absorption near-edge structure) spectroscopy[a].

Sample	pH	Loading rate (mmol kg^{-1})	Peak 'a' (TEY)[b]		Peak 'a' (FY)[c]		Peak 'a' TEY: Peak 'a' FY Ratio
			Height[d]	Position (eV)	Height[e]	Position (eV)	
1	7.0	525.95	6.15	193.99	7.49	194.00	0.82
2	7.0	1654.19	8.70	193.99	10.51	193.99	0.83
3	7.0	1913.95	9.23	193.99	12.31	193.99	0.75
4	9.2	874.07	6.97	193.96	7.65	194.04	0.91
5	9.2	2068.58	10.10	193.99	9.74	193.99	1.04
6	9.2	2782.15	14.53	193.99	12.63	193.99	1.15

[a]All samples contain ionic strength = 0.1 M NaCl.
[b]TEY (total electron yield).
[c]FY (fluorescence yield).
[d]Height of peak 'a' in TEY-XANES spectra linearly correlated with B loading rate with a $R^2 = 0.9051$.
[e]Height of peak 'a' in FY-XANES spectra linearly correlated with B loading rate with a $R^2 = 0.7993$.

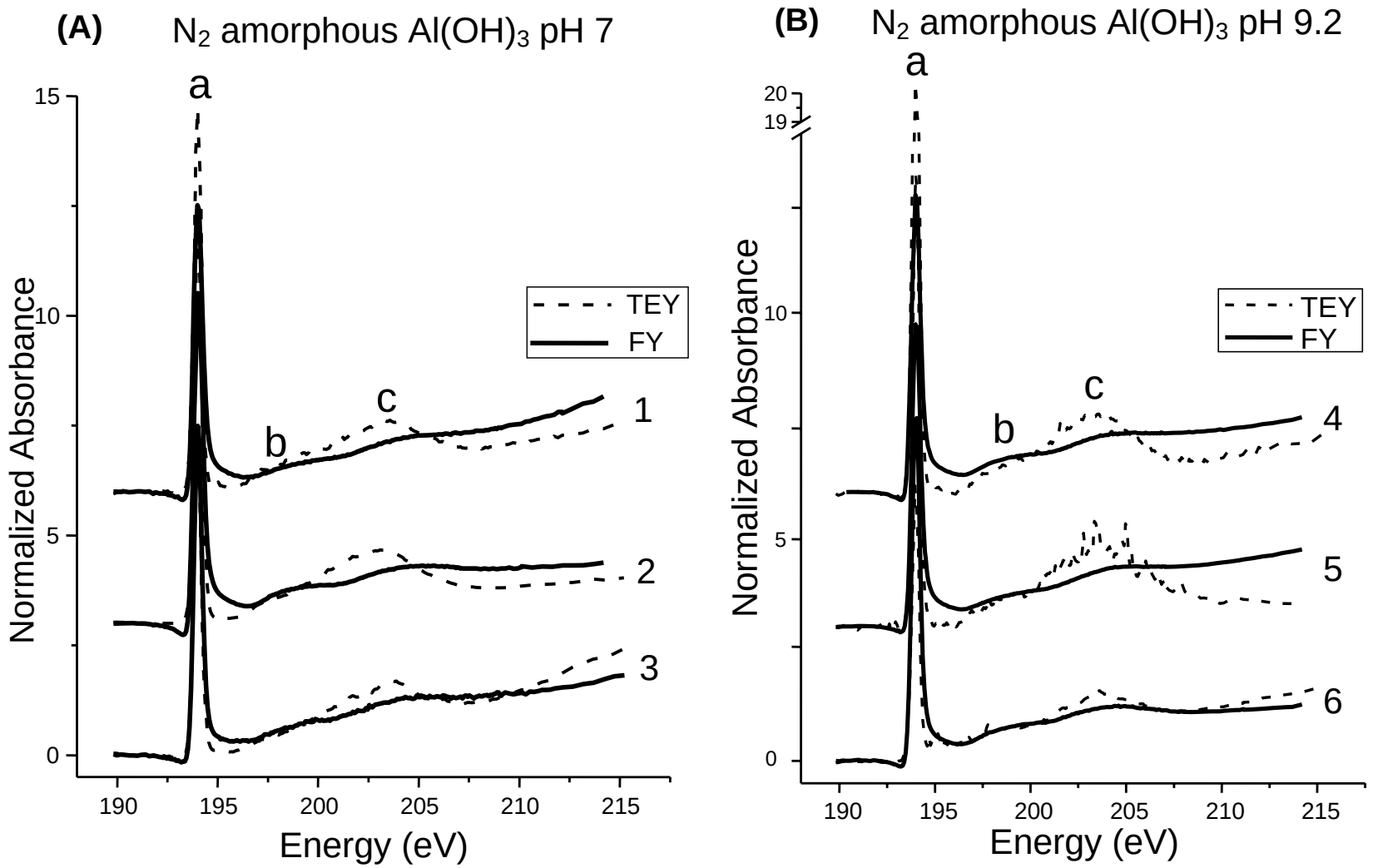

Figure 4.3 B *K*-edge XANES spectra of boric acid adsorption on am-$Al(OH)_3$. (A) Conducted at pH 7 under N_2 condition and (B) conducted at pH 9.2 under N_2 condition. Detailed sample information and loading rate are provided in Table 4.1.

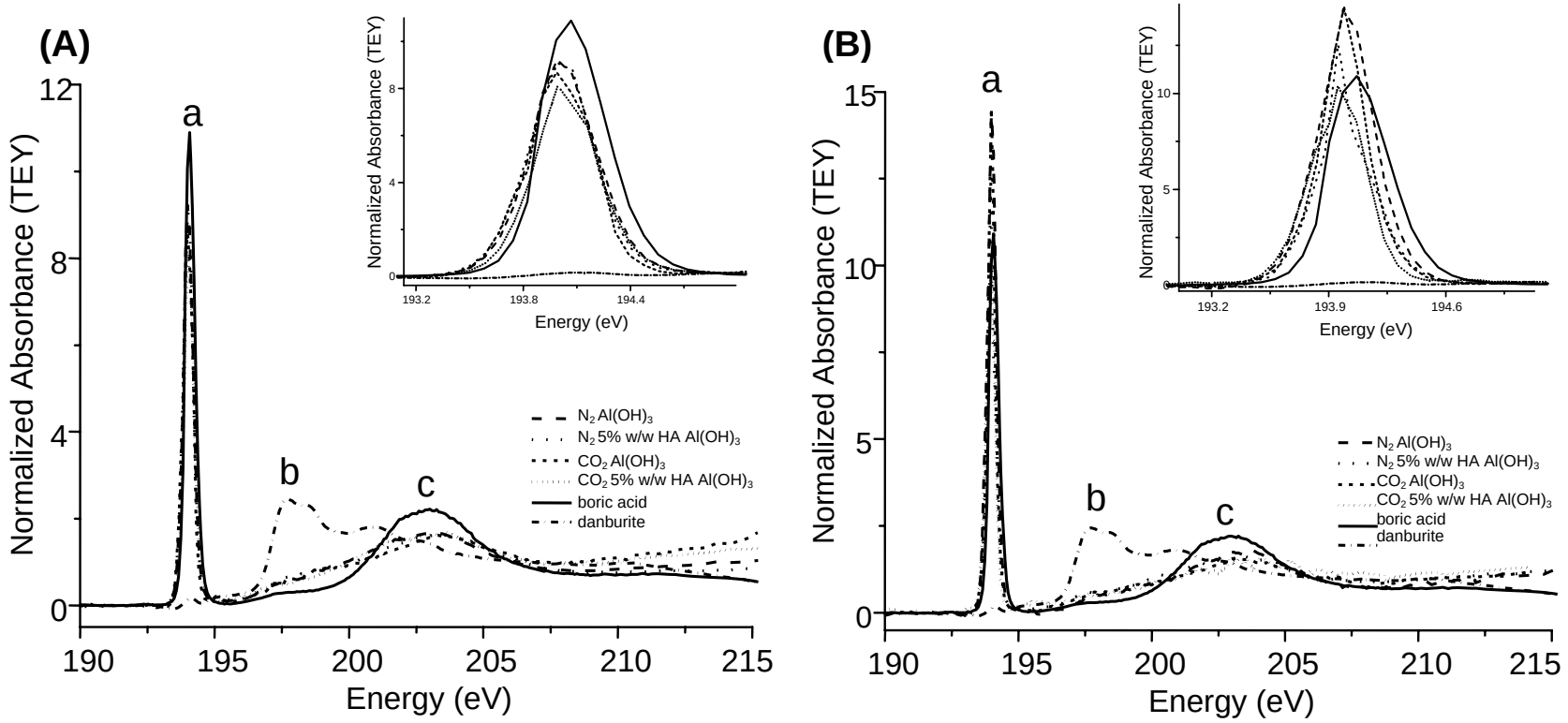

Figure 4.4 B *K*-edge TEY-XANES spectra of boric acid adsorption isotherm samples. (A) Conducted at pH 7.0 and expanded view of peak 'a'. (B) Conducted at pH 9.2 and expanded view of peak 'a'. Detailed sample information and loading rate are provided in Table 4.2.

Table 4.2 Boric acid adsorption isotherm freeze dried paste samples analyzed by B *K*-edge XANES (X-ray absorption near-edge structure) spectroscopy[a].

Sample		pH	Loading rate (mmol kg^{-1})	Decrease in loading rate (%)[e]	Peak 'a' (FY)[b]		Decrease in Peak 'a' (FY) (%)[e]	Peak 'a' (TEY)[c]		Decrease in Peak 'a' (TEY) (%)[e]
					Height	Position (eV)		Height[d]	Position (eV)	
1	N_2 - $Al(OH)_3$	9.2	2782.1	N/A	7.72	194.04	N/A	14.53	193.99	N/A
2	N_2 - 5% w/w HA $Al(OH)_3$	9.2	2442.4	12.21	7.16	194.04	7.25	12.55	193.96	13.63
3	CO_2 - $Al(OH)_3$	9.2	2745.8	1.30	7.67	193.99	0.64	14.34	193.99	1.31
4	CO_2 - 5% w/w HA $Al(OH)_3$	9.2	1983.9	28.69	6.39	193.99	17.23	10.38	193.95	28.56
5	N_2 - $Al(OH)_3$	7.0	1654.2	N/A	7.78	193.99	N/A	9.23	193.99	N/A
6	N_2 - 5% w/w HA $Al(OH)_3$	7.0	1585.5	4.15	7.65	194.04	1.67	9.08	193.99	1.63
7	CO_2 - $Al(OH)_3$	7.0	1633.2	1.27	7.70	193.99	1.03	8.70	193.99	5.74
8	CO_2 - 5% w/w HA $Al(OH)_3$	7.0	1231.1	25.58	6.42	193.99	17.48	8.13	193.99	11.92
9	boric acid	N/A	N/A	N/A	6.87	194.07	N/A	10.90	194.07	N/A
10	danburite	N/A	N/A	N/A	0.035	194.08	N/A	0.16	194.08	N/A

[a]All samples contain $[B(OH)_3]_{tot}$ = 50 mmol L^{-1} and ionic strength = 0.1 M NaCl.
[b]FY (fluorescence yield).
[c]TEY (total electron yield).
[d]Height of peak 'a' in TEY-XANES spectra linearly correlated with B loading rate with a R^2 = 0.9256.
[e]Calculated with respected to the N_2 – $Al(OH)_3$ sample at the corresponding pH.

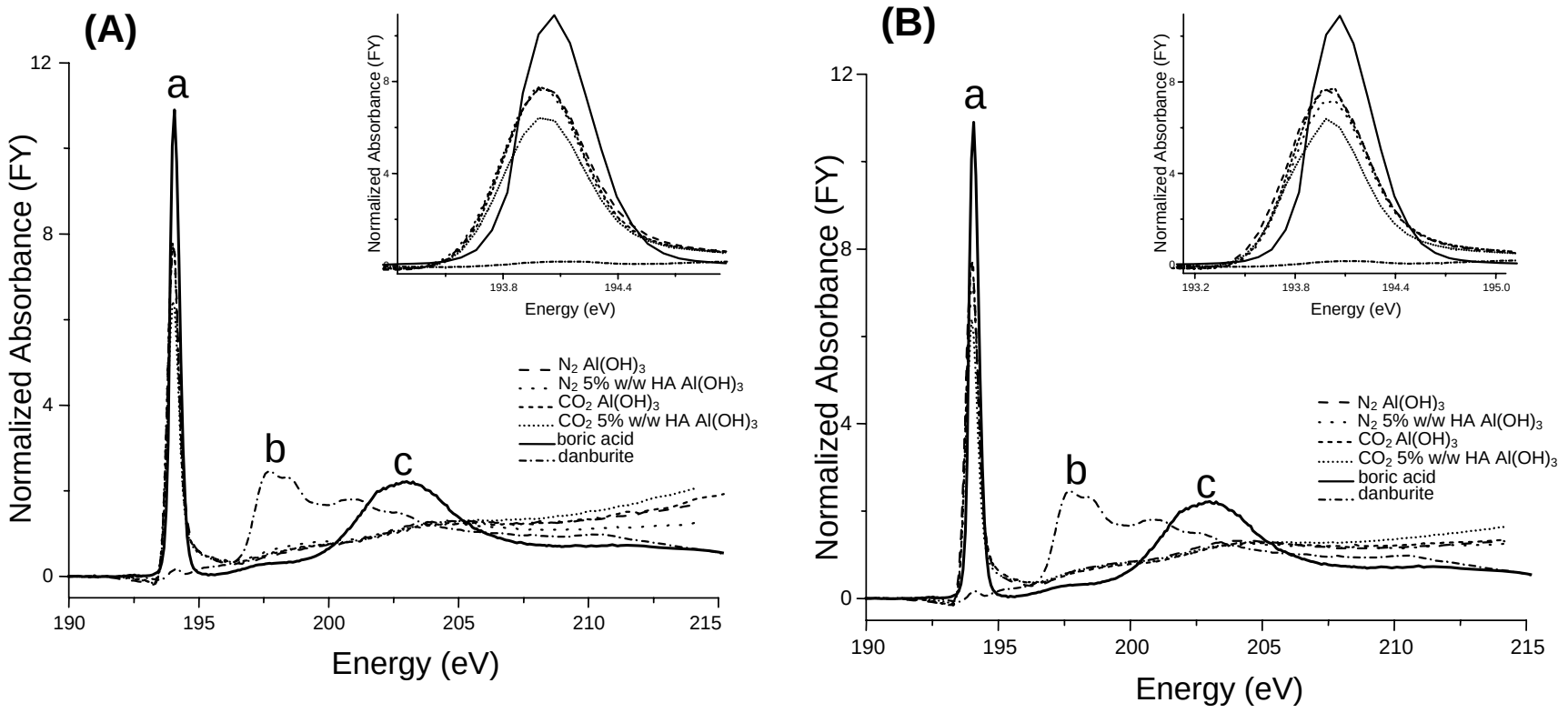

Figure 4.5 B *K*-edge FY-XANES spectra of boric acid adsorption isotherm samples. (A) Conducted at pH 7.0 and expanded view of peak 'a'. (B) Conducted at pH 9.2 and expanded view of peak 'a'. Detailed sample information and loading rate are provided in Table 4.2.

was found to be linearly correlated to B loading rate (R^2 = 0.9256), furthermore the percentage decrease in the height of peak 'a' corresponded to the percent decrease in B loading rate (Table 4.2). The combined effects of HA complexation with am-$Al(OH)_3$ and dissolved CO_2 resulted in the largest reduction in the proportion of trigonally coordinated B complexes (the height of peak 'a') at both pH 7.0 and 9.2 (see inset, Figure 4.4 and 4.55).

In both TEY and FY-XANES spectra, a slight downshift in the energy of peak 'a' was observed in all of the adsorption samples compared to standards (Table 4.2). The shift of energy in peak 'a' can be attributed to inner-sphere complexation between boric acid with pure and coated mineral. The presence of peak 'b' in the adsorption samples showed that tetrahedrally coordinated B complexes were present (Figure 4.4 and 4.5). Most of the tetrahedral $B(OH)_4^-$ complexes are assumed to be inner-sphere, as outer-sphere interactions (hydrogen bonding, long-range electrostatic) are unlikely to occur when the pH is above the PZC of the mineral.

4.4. Conclusion

Based on results from macroscopic adsorption studies and B *K*-edge XANES spectroscopy, we conclude that boric acid forms inner-sphere trigonal $B(OH)_3$ complexes with am-$Al(OH)_3$ and HA coated am-$Al(OH)_3$ at neutral and alkaline pH values. Inner-sphere tetrahedral $B(OH)_4^-$ species are present, however the proportion of these species remains relatively low compared to trigonal $B(OH)_3$. Although not explicitly considered in the analysis, it is unlikely that boric acid or a borate group could interact with dissolved CO_2 to form $B(OH)_2CO_3^-$ in the am-$Al(OH)_3$ system. However, the occurrences of these boric acid-carboxyl complexes might be possible in the HA system, as fewer OH- sites from the mineral would be available for binding. Regardless of these possible complexes, the primary effect inorganic and organic carbon for this system is a significant decrease in boric acid adsorption in systems combining dissolved CO_2 and HA.

Much research emphasis has been placed on the study of boric acid-organic acid (i.e. HA) complexation (Gu and Lowe, 1990; Lemarchand et al., 2005). The results from this study suggest that future HA complexation studies may be different if one

considers a ternary boric acid-humic acid-mineral system. These aggregate surfaces are extremely common in soils, as HAs are naturally found adsorbed to soil mineral aggregated surfaces (Tombacz et al., 1997; Schnitzer and Schulten, 1998). Furthermore, this study shows that HA is a much weaker adsorbent than am-$Al(OH)_3$, hence HA coating decreased sorption of boric acid.

Additionally, since the soil gas phase has a markedly higher CO_2 content relative to the atmosphere (Sposito, 1989), the results from this study, as well as studies conducted by Wijnja and Schulthess (Wijnja and Schulthess, 2000; Wijnja and Schulthess, 2002), suggest the inclusion of dissolved CO_2 species in future oxyanion sorption studies.

5. GENERAL DISCUSSION AND CONCLUSIONS

Similar to studies conducted with other oxyanions (sulfate, selenate and arsenate), this dissertation also found that a mixture of surface complexation mechanisms occur, and that the relative inner-sphere to outer-sphere borate adsorption on the mineral is dependent on pH, ionic strength and the presence of other competitive ions. The formation of outer- and inner-sphere boric acid complexes is not unexpected as previous studies have confirmed this anomaly (Su and Suarez, 1995; Peak et al., 2002). This bonding mechanism could potentially be applied to other neutral compounds (arsenite) when studying the sorption process in the environment.

In summary, the present study on the influence of HA on boric acid adsorption by am-$Al(OH)_3$ mineral suggests that complexation studies should be validated under more natural conditions. In natural systems, HAs are normally found associated with soil mineral surfaces (Tombacz et al., 1997; Schnitzer and Schulten, 1998). In this study, the competitive effect between boric acid and HA for adsorption sites on minerals is much more important than the potential complexation of boric acid with HA. In the future, the interaction between minerals and organic acids should be considered when investigating the coordination of boric acid and other oxyanions in a complex heterogeneous environment.

Although vibrational spectroscopy was not successful in identifying any B complexes in humic substances, it did prove to be a rigorous method of identifying tetrahedrally and trigonally coordinated complexes on am-$Al(OH)_3$. B *K*-edge XANES Spectroscopy was an effective tool in determining the speciation of B complexes in mineral and adsorption samples. However, further development of soft X-ray absorption spectroscopy is needed to extend this method to hydrated samples to better characterize the sorption processes in aqueous systems.

This dissertation has confirmed HA coating on am-$Al(OH)_3$ (either via direct competition and/or surface modification) can decrease adsorption of boric acid. The effect other organic acids (fulvic and various low molecular weight organic acids) may

have on boric acid adsorption still remains unknown. The type and concentration of the organic acid present in the system will likely play an important role in governing sorption capability. Future adsorption studies that incorporate drying-wetting cycles as well as freezing-thawing cycles will also help to shed light on the how physiochemical alteration of the mineral surface will affect the sorption/desorption of oxyanions.

The studies carried out for this dissertation were conducted with one oxyanion on two types of adsorbents under constant ionic strength. The actual system in nature is expected to be more complex with various other metals, oxyanions and organic acids involved in the sorption process. However, the knowledge obtained from this dissertation will help further the understanding boric acid chemistry in the environment with the ultimate goal of decoding the surface chemistry of soils.

6. REFERENCE

Afif, E., V. Barron, and T. Torrent. 1995. Organic matter delays but does not prevent phosphate sorption by cerrado soils from Brazil. Soil Sci. 159:207-211.

Alvarez, R., and D.L. Sparks. 1985. Polymerization of silicate anion in solutions at low concentrations. Nature 318:649-651.

Ascerbo, S., R. Kastori, S. H, H. Harms, and K. Haider. 1973. Effect of boron on synthesis and transformation of lignin precursors in *Zea mays*. Z. Pflanzenphysiol. 69:306-317.

Baas Becking, L.G.M., I.R. Kaplan, and D. Moore. 1960. Limits of the nautral environment in temrs of plant and oxidation-reduction potentials. J. Geol. 68:243-284.

Baia, L., R. Stefan, W. Kiefer, and S. Simon. 2005. Structural characteristics of B_2O_3-Bi_2O_3 glasses with high transition metal oxide content. Journal of Raman Spectroscopy 36:262-266.

Barrow, N.J. 1989. Testing a mechanistic model. The effect of pH and electrolyte concentration on borate sorption by a soil. J. Soil Sci. 40:427-435.

Berger, K.C., and E. Truog. 1939. Boron determination in soils and plants using the quinalizarin reaction. Ind. Eng. Chem. 11:540-545.

Bertsch, P.M., and D.R. Parker. 1996. Aqueous polynuclear aluminum species, *In* G. Sposito, ed. The Environmental Chemistry of Aluminum. CRC/Lewis Publisher, Boca Raton, FL.

Beyrouty, C.A., G.E. Van Scoyoc, and J.R. Feldkamp. 1984. Evidence supporting specific adsorption of boron on synthetic aluminum hydroxide. Soil Sci. Soc. Am. J. 48:284-287.

Bhatnagar, R.S., S.C. Attri, G.S. Mathur, and R.S. Chaudhary. 1979. Boron adsorption equilibrium in soils. Ann. Arid Zone 18:86-95.

Biggar, J.W., and M. Fireman. 1960. Boron adsorption and release by soils. Soil Sci. Soc. Am. J. 24:115-120.

Bingham, F.T. 1982. Boron., p. 431-447, *In* A. L. Page, ed. Methods of Soil Analysis, Part 2. Chemical and Microbiological Properties, 2nd ed. ASA and SSSA, Madison, WI.

Bingham, F.T., A.L. Page, N.T. Colemand, and K. Flach. 1971. Boron adsorption characteristics of selected soils from Mexico and Hawaii. Soil Sci. Soc. Am. J. 35:546-550.

Bloesch, P.M., L.C. Bell, and J.D. Hughes. 1987. Adsorption and desorption of boron by goethite. Aust. J. Soil Res. 25:377-390.

Bohn, H.L., B.L. McNeal, and G.A. O'Connon. 1979. Soil Chemistry John Wiley & Sons, New York.

Brydson, R., D.D. Vvedensky, W. Engel, H. Sauer, B.G. Williams, E. Zeitler, and J.M. Thomas. 1988. Chemical information from electron-energy-loss near-edge structure: core hole effects in the beryllium and boron *K*-edges of rhodizite. J. Phys. Chem. 92:962-966.

Choi, W.W., and K.Y. Chen. 1979. Evaluation of boron removal by adsorption on solids. Environ. Sci. Technol. 13:189-196.

Chrisholm-Brause, C.J., P.A. O'Day, G.E. Brown, and G.A. Parks. 1990. Evidence of multinuclear metal-ion complexes at solid/water interfaces from X-ray absorption spectroscopy. Nature 348:528-531.

Cotton, F.A., and G. Wilkinson. 1989. Advance Inorganic Chemistry. 5th ed. Wiley, New York.

Couch, E.L., and R.E. Grim. 1968. Boron fixation by illites. Clays Clay Miner. 16:249-256.

Duff, M.C., and C. Amrhein. 1996. Uranium (VI) adsorption on goethite and soil in carbonate solution. Soil Sci. Soc. Am. J. 60:1393-1400.

Edwards, J.O., G.C. Morrison, V.F. Ross, and J.W. Schultz. 1954. The structure of the aqueous borate ion. J. Am. Chem. Soc. 77:266-268.

El-Motaium, R., H. Hu, and P.H. Brown. 1994. The relative tolerance of six *Prunus* rootstocks to boron and salinity. J. Am. Soc. Hortic. Sci. 119:1169-1175.

Elrashidi, M.A., and G.A. O'Connor. 1982. Boron sorption and desorption in soils. Soil Sci. Soc. Am. J. 46:27-31.

Fendorf, S., D.L. Sparks, G.M. Lamble, and M.J. Kelley. 1994. Applications of X-ray absorption fine structure spectroscopy to soils. Soil Sci. Soc. Am. J. 58:1583-1595.

Fleet, M.E. 1965. Preliminary investigations into the sorption of boron by clay minerals. Clay Miner. 6:3-16.

Fleet, M.E., and S. Muthupari. 2000. Boron *K*-edge XANES of borate and borosilicate minerals. Am. Mineral. 85:1009-1021.

Fleet, M.E., and X. Liu. 2001. Boron *K*-edge XANES of boron oxides: tetrahedral B-O distances and near-surface alteration. Phys. Chem. Miner. 28:421-427.

Fleming, G.A. 1980. Essential micronutrients. I: boron and molydenum, p. 155-197, *In* B. E. Davies, ed. Applied Soil Trace Elements. John Wiley and Sons, New York.

Garvie, L.A.J., A.J. Craven, and R. Brydson. 1995. Parallel electron energy-loss spectroscopy (PEELS) study of B in minerals: The electron energy-loss near-edge structure (ELNES) of the B *K* edge. Am. Mineral. 80:1130-114.

Goldberg, S. 1997. Reactions of boron with soils. Plant and Soil 193:35-48.

Goldberg, S. 1999. Reanalysis of boron adsorption on soils and soil mineral using the Constant Capacitance model. Soil Sci. Soc. Am. J. 63:823-829.

Goldberg, S. 2005. Inconsistency in the triple layer model description of ionic strength dependent boron adsorption. J. Colloid Interface Sci. 285:509-517.

Goldberg, S., and R.A. Glaubig. 1985. Boron adsorption on aluminum and iron oxide minerals. Soil Sci. Soc. Am. J. 49:1374-1379.

Goldberg, S., and R.A. Glaubig. 1986a. Boron adsorption on California soils. Soil Sci. Soc. Am. J. 50:1173-1176.

Goldberg, S., and R.A. Glaubig. 1986b. Boron adsorption and silicon release by the clay minerals kaolinite, montmorillonite, and illite. Soil Sci. Soc. Am. J. 50:1442-1448.

Goldberg, S., and R.A. Glaubig. 1988. Boron and silicon adsorption on an aluminum oxide. Soil Sci. Soc. Am. J. 52:87-91.

Goldberg, S., H.S. Forster, and E.L. Heick. 1993a. Boron adsorption mechanisms on oxides, clay minerals, and soil inferred from ionic strength effects. Soil Sci. Soc. Am. J. 57:704-708.

Goldberg, S., H.S. Forster, and E.L. Heick. 1993b. Temperature effects on boron adsorption by reference minerals and soils. Soil Science 156:316-321.

Goldberg, S., H.S. Forster, and E.L. Heick. 1993c. Temperature effects on boron adsorption by reference minerals and soils. Soil Sci. 156:316-321.

Goldberg, S., H.S. Forster, S.M. Lesch, and E.L. Heick. 1996. Influence of anion competition on boron adsorption by clays and soils. Soil Sci. Soc. Am. J. 161:99-103.

Goldberg, S., I. Lebron, D.L. Suarez, and Z. Hinedi. 2001. Suface characterization of amorphous aluminum oxides. Soil Sci. Soc. Am. J. 65:78-86.

Goldberg, S., D.L. Suarez, N.T. Basta, and S.M. Lesch. 2004. Predicting boron adsorption isotherms by Midwestern soils using the Constant Capacitance model. Soil Science Society of America Journal 68:795-801.

Greenwood, N.N., and A. Earnshaw. 1984. Chemistry of the Elements Pergamon Press, New York.

Gu, B., and L.E. Lowe. 1990. Studies of the adsorption of boron on humic acids. Can. J. Soil Sci. 70:305-311.

Gu, B., J. Schmitt, Z. Chen, L. Liang, and J.F. McCarthy. 1994. Adsorption and desorption of natural organic matter on iron oxides: mechanism and models. Environ. Sci. Technol. 28:38-46.

Gupta, U.C. 1968. Relationship of total and hot-water soluble boron, and fixation of added B, to properties of podzol soils. Soil Sci. Soc. Am. J. 32:45-48.

Gupta, U.C. 1993. Boron and its Role in Crop Production CRC Press, Boca Raton, Fl.

Gupta, U.C., and J.A. MacLeod. 1977. Influence of calcium and magnesium sources on boron uptake and yield of alfalfa and rutabaga as it related to soil pH. Soil Sci. 124:279-284.

Hallmeier, K.H., R. Szargan, A. Meisel, E. Hartmann, and E.S. Gluskin. 1981. Investigation of core-excited quantum yield spectra of high-symmetric boron compounds. Spectrochim. Acta.

Harada, T., and M. Tamai. 1968. Some factors affecting behaviour of boron in soil. I. Some soil properties affecting boron adsorption of soil. J. Plant Nutr. 14:215-224.

Hatcher, J.T., C.A. Bower, and M. Clark. 1967. Adsorption of boron by soils as influenced by hydroxy aluminum and surface area. Soil Sci. 104:422-426.

Hibben, J.H. 1939. The Raman Effect and its Chemical Applications Reinhold Publishing Corporation, New York, NY.

Hingston, F.J. 1964. Reactions between boron and clays. Aust. J. Soil Res. 2:83-95.

Hsu, P.H. 1989. Aluminum hydroxides and oxyhydroxides, p. 331-378, *In* J. B. Dixon and S. W. Weed, eds. Minerals in Soil Environment. Soil Science Society of America, Madison, WI.

Huang, P.M. 1988. Ionic factors affecting aluminum transformations and the impact on soil and environmental sceinces. Adv. Soil Sci. 8:1-78.

Huang, P.M. 1991. Organo-alumino polymer associations and their significance in soil and environmental sciences, p. 179-237, *In* M. De Boodt, et al., eds. Soil Colloids and their Association in Aggregates. Plenum Press, New York.

Huang, P.M., M.K. Wang, N. Kampf, and D.G. Schulze. 2002. Aluminum hydroxides Soil Mineralogy with Environmental Applications. Soil Science Society of America, Madison, WI.

Huettl, P.J.V. 1976. The pH dependent sorption of boron by soil organic matter. M.Sc., Univeristy of Wisconsin, Madison, Wisconsin, USA.

Hunter, R. 1988. Zeta Potential In Colloid Science: Principles and Applications. Academic Press, London, UK.

Hunter, R.J. 1981. Zeta Potential in Colloid Science Academic Press, New York, USA.

Iliescu, T., I. Adrelean, V. Simon, and D. Maniu. 1995. Raman study of B_2O_3-PbO-Nd_2O_3 glasses. Journal of Materials Science Letters 14:393-395.

Ishiguro, E., S. Iwata, Y. Suzuki, A, and T. Sasaki. 1982. The boron K photoabsorption spectra of BF_3, BCl_3, and BBr_3. J. Phys. 15B:1841-1854.

Jasmund, K., and B. Lindner. 1973. Experiments on the fixation of boron by clay minerals. Proceedings of the International Clay Conference 1972:399-412.

Kasrai, M., Z. Yin, G.M. Bancroft, and K. Tan. 1993. X-ray fluorescence measurements of x-ray absorption near edge structure at the Si, P and S *L* edges. J. Vac. Sci. Technol. A. 11:2694-2699.

Kasrai, M., M.E. Fleet, S. Muthupari, D. Li, and G.M. Bancroft. 1998. Surface modification study of borate material from B *K*-edge X-ray absorption spectroscopy. Phys. Chem. Miner. 25:268-272.

Keren, R., and U. Mezuman. 1981. Boron adsorption by soils using a phenomenological adsorption equation. Soil Sci. Soc. Am. J. 45:722-726.

Keren, R., and R.G. Gast. 1981. Effects of wetting and drying, and exchangeable cations, on boron adsorption and realease by montmorillinite. Soil Sci. Soc. Am. J. 45:478-482.

Keren, R., and G.A. O'Connon. 1982. Effect of exchangeable ions and ionic strength on boron adsorption by montmorillonite and illite. Clays Clay Miner. 30:341-346.

Keren, R., and H. Talpaz. 1984. Boron adsorption by montmorillinite as affected by particle size. Soil Sci. Soc. Am. J. 48:555-595.

Keren, R., and F.T. Bingham. 1985. Boron in water, soils and plants, p. 291-276 Advances in Soil Science, Vol. 1. Springer-Verlag, New York.

Keren, R., and D.L. Sparks. 1994. Effect of pH and ionic strength on boron adsorption by pyrophyllite. Soil Sci. Soc. Am. J. 58:1095-1100.

Keren, R., R.G. Gast, and B. Bar-Yosef. 1981. pH-dependent boron adsorption by Na-montmorillonite. Soil Sci. Soc. Am. J. 45:45-48.

Keren, R., F.T. Bingham, and J.D. Rhoades. 1985. Plant uptake of boron as affected by boron distribution bewteen liquid and solid phases in soil. Soil Sci. Soc. Am. J. 49:297-302.

Keren, R., P.R. Grossl, and D.L. Sparks. 1994. Equilibrium and kinetics of borate adsorption-desorption on pyrophyllite in aqueous suspensions. Soil Sci. Soc. Am. J. 58:1116-1122.

Khare, N., D. Hesterberg, and J. Martin. 2005. XANES investigation of phosphate sorption in single and binary systems of iron and aluminum oxide minerals. Environ. Sci. Technol. 39:2152-2160.

Koningsberger, D.C., and R. Prins. 1988. X-ray Absorption: Principles, Applications, Techniques of EXAFS, SEXAFS and XANES John Wiley & Sons, New York.

Krauskopf, K.B. 1972. Geochemistry of micronutrients, *In* J. Mortvedt, et al., eds. Micronutrients in Agriculture. Soil Science Society of America, Madison, Wisconsin, USA.

Kwong, K.F., and P.M. Huang. 1979. Surface reactivity of aluminum hydroxides precipitated in the presence of low-moleculare-weight organic acids. Soil Sci. Soc. Am. J. 43:1107-1113.

Lehto, L. 1995. Boron retention in limed forest mor. For. Ecol. Manage. 78:11-20.

Lemarchand, E., J. Schott, and J. Gaillardet. 2005. Boron isotopic fractionation related to boron sorption on humic acid and the structure of surface complexes formed. Geochim. Cosmochim. Acta 69:3519-3533.

Li, D., G.M. Bancroft, and M.E. Fleet. 1996. B *K*-edge XANES of crystalline and amorphous inorganic materials. J. Electron Spectrosc. Relat. Phenom. 79:71-73.

Liu, Z., B. Gao, M. Hu, S. Li, and S. Xia. 2003. FT-IR and Raman spectroscopic analysis of hydrated cesium borate and their saturated aqueous solution. Spectrochim. Acta 59:2741-2745.

Liu, Z., B. Gao, S. Li, M. Hu, and S. Xia. 2004. Raman spectroscopic analysis of supersaturated aqueous solution of $MgOB_2O_3$-32%$MgCl_2$-H_2O during acidification and dilution. Spectrochimica Acta Part A 60:3125-3128.

Maeda, M., T. Hirao, M. Kotaka, and H. Kakihana. 1979. Raman spectra of polyborate ions in aqueous solution. Journal of Inorganic and Nuclear Chemistry 41:1217.

Malcolm, R.L., and P. MacCarthy. 1986. Limitations in the use of commerical humic acids in water and soil research. Environ. Sci. Technol. 20:904-911.

Maniu, D., T. Iliescu, I. Ardelean, R. Ciceo-Lucacel, M. Bolboaca, and W. Kiefer. 2002. Raman study of B_2O_3-SrO-CuO glasses. Vib. Spec. 29:241-244.

Marinsky, J.A., S. Gupta, and P. Schindler. 1982. The interaction of Cu(II) ion with humic acid. J. Colloid Interface Sci. 89:401-411.

Marzadori, C., L. Vittori Antisari, C. Ciavatta, and P. Sequi. 1991. Soil organic matter influence on adsorption and desorption of boron. Soil Sci. Soc. Am. J. 55:1582-1585.

Mattigod, S.V., J.A. Pframpton, and C.H. Lim. 1985. Effect of ion-pair formation on boron adsorption by kaolinite. Clays Clay Miner. 33:433-437.

Maya, L. 1976. Identification of polyborate and fluoropolyborate ions in solution by Raman spectroscopy. Inorg. Chem. 15:2179-2184.

McBride, M.B. 1997. A critique of diffuse double layer models applied to colloid and surface chemistry. Clays Clay Miner. 45:598-608.

McPhail, M., A.L. Page, and F.T. Bingham. 1972. Adsorption interactons of monosilicic and boric acid on hydrous oxides of iron and aluminum. Soil Sci. Soc. Am. Proc. 36:510-514.

Morgan, V. 1980. Boron Geochemistry, *In* Mellor, ed. Mellor's Comprehensive Treaties on Inorganic and Theoretical Chemistry, Vol. V, Part A: Boron-Oxygen Compounds. Longman, New York.

Nable, R.O., G.S. Banuelos, and J.G. Paull. 1997. Boron toxicity. Plant Soil 193:181-198.

Nakamoto, K. 1997. Infrared and Raman Spectra of Inorganic and Coordination Compounds - Part A: Theory and Application in Inorganic Chemistry. John Wiley and Sons, Inc, New York, NY.

Okude, N., M. Nagoshi, H. Noro, Y. Baba, H. Yamamoto, and T. Sasaki. 1999. P and S *K*-edge XANES of transition-metal phosphates and sulfates. J. Electron. Spectrosc. 101-103:607-610.

Olson, R.V., and K.C. Berger. 1946. Boron fixation as influenced by pH, organic matter content, and other factors. Soil Sci. Soc. Am. Proc. 11:216-220.

Park, W.L., and J.L. White. 1952. Boron retention by clay and humus systems saturated with various cations. Soil Sci. Soc. Am. J. 16:298-300.

Parr, A.J., and B.C. Loughman. 1983. Boron and membrane function in plants, p. 87-107, *In* D. A. Robb and W. S. Pierpoint, eds. Metals and Micronutrients: Uptake and Utilization by Plants. Academic Press, New York.

Peak, D., R.G. Ford, and D.L. Sparks. 1999. An in situ ATR-FTIR investigation of sulfate bonding mechanisms on goethite. J. Colloid Interface Sci. 218:289-299.

Peak, D., G.W. Luther, and D.L. Sparks. 2002. ATR-FTIR spectroscopic studies of boric acid adsorption on hydrous ferric oxide. Geochim. Cosmochim. Acta 67:2551-2560.

Perdue, E.M. 1988. Measurements of binding site concentrations in humic substances, p. 135-154, *In* J. R. Kramer and H. E. Allen, eds. Metal Speciation: Theory, Analysis and Application. Lewis Publishers, Chelsea, Michigan.

Pizer, R., and P. Ricatto. 1994. Ternary alkaline earth metal complex ions in the M^{2+}/borate/tartrate system as studied by ^{11}B NMR. Inorg. Chem. 33:4985-4990.

Porrenga, D.H. 1967. Influence of grinding and heating of layer silicates on boron sorption. Geochim. Cosmochim. Acta 31.

Prange, A., and H. Modrow. 2002. X-ray absorption spectroscopy and its application in biological, agricultural and environmental research. Rev. Environ. Sci. Bio. Tech. 1:259-276.

Preston, H.J.T., J.J. Kaufman, J. Keller, and J.B. Danese. 1976. MS-Xα calculations on boron trihalides and comparison with their photoelectron spectra. Chem. Phys. Lett. 37:55-59.

Reininger, R., K. Tan, and I. Coulthard. 2002. An insertion device beamline for 5-250 eV at the Canadian Light Source. Rev. Sci. Instrum. 73:1489-1591.

Reisenauer, H.M., L.M. Walsh, and R.G. Hoeft. 1973. Testing soils for sulphur, boron, molybdenum, and chlorine, *In* L. M. Walsh and J. D. Beaton, eds. Soil Testing and Plant Analysis. Soil Science Society of America Inc, Madison, WIsconsin, USA.

Reuter, J.H., and E.M. Perdue. 1977. Importance of heavy metal-organic matter interactions in natural water. Geochim. Cosmochim. Acta 41:325-334.

Schalscha, E.B., F.T. Bingham, G.G. Galindo, and H.P. Galvan. 1973. Boron adsorption by volcanic ash soils in Southern Chile. Soil Sci. 116:70-76.

Schnitzer, M. 1965. The application of infrared spectroscopy to investigations of soil humic compounds. Can. J. Spectrosc. 10:121-127.

Schnitzer, M., and S.I.M. Skinner. 1965. Organo-metallic interactions in soils: 4. Carboxyl and hydroxyl groups in organic matter and metal retention. Soil Sci. 99:278-284.

Schnitzer, M., and H. Schulten. 1998. New ideas on the chemical make-up of soil humic and fulvic acids, p. 153-177, *In* P. M. Huang, ed. Future Prospects for Soil Chemistry. Soil Science Society of America, Madison, WI.

Schulthess, C.P., and J.F. McCarthy. 1990. Competitive adsorption of aqueous carbonic and acetic acids by an aluminum oxide. Soil Sci. Soc. Am. J. 54:688-694.

Schulze, D.G. 2002. An introduction to soil mineralogy, p. 1-20, *In* J. B. Dixon and D. G. Schulze, eds. Soil mineralogy with environmental applications. SSSA, Madison, WI.

Schwarz, W.H.E., L. Mensching, K.H. Hallmeier, and R. Szargan. 1983. *K*-shell excitationns of BF_3, CF_4, and MBF_4 compounds. Chemical Physics 82:57965.

Shorrocks, V.M. 1997. The occurrence and correction of boron deficiency. Plant Soil 193:121-148.

Shriver, D., and P. Atkins. 1994. Inorganic Chemistry Oxford University Press, Oxford.

Sims, J.R., and F.T. Bingham. 1967. Retention of boron by layer silicates, sesquioxides, and soil materials: I. Layer silicates. Soil Sci. Soc. Am. J. 32:364-369.

Sims, J.R., and F.T. Bingham. 1968. Retention of boron by layer silicates, sesquioxides, and soil materials: II. Sesquioxides. Soil Sci. Soc. Am. J. 32:364-373.

Singh, M. 1971. Equilibrium adsorption on boron in soils and clays. Geoderma 5:209-217.

Sparks, D.L. 2003. Environmental Soil Chemistry. 2nd ed. Academic Press, London.

Spiers, G.A., M.J. Dudas, and L.W. Hodgins. 1983. Simultaneous multielement analysis of clays by inductively coupled plasma-atomic emission spectroscopy using suspension aspiration. Clays Clay Miner. 31:397-400.

Sposito, G. 1989. The Chemistry of Soils. Oxford University Press, New York, NY.

Stohr, J. 1992. NEXAFS Spectroscopy Springer Series in Surface Sciences, Vol. 25. Springer-Verlag, Berlin.

Stumm, W. 1992. Chemistry of the Solid-Water Interface: Processes at the Mineral-Water and Particle-Water Interface in Natural Systems Wiley, New York.

Su, C., and D.L. Suarez. 1995. Coordination of adsorbed boron: a FTIR spectroscopy study. Environ. Sci. Technol. 29:302-311.

Su, C., and D.L. Suarez. 1997. Boron sorption and release by allophane. Soil Sci. Soc. Am. J. 61:69-77.

Swift, R.S. 1996. Organic matter characterization, p. 1018-1020, *In* D. L. Sparks, ed. Methods of soil analysis, Vol. Book Series: 5. Soil Science Society of America, Madison, WI.

Tombacz, E., J.A. Rice, and S. Ren. 1997. Humic and Fulvic Acids, p. 43-50, *In* J. Drozd, et al., eds. The Role of Humic Substance in the Ecosystems and in Environmental Protection. IHSS-Polish Society of Humic Sustances, Wroclaw, Poland.

Tossell, J.A. 1986. Studies of unoccupied molecular orbital calculations, X-ray absorption near edge, electron transmissions, and NMR spectroscopy. Am. Mineral. 71:1170-1177.

Van Green, A., A.P. Robertson, and J.O. Leckie. 1994. Complexation of carbonate species at the goethite surface: implication for adsorption of metal ions in natural waters. Geochim. Cosmochim. Ac. 58:2073-2086.

van Raij, B., and M. Peech. 1972. Electrochemical properties of some Oxisols and Alfisols of the tropics. Soil Sci. Soc. Am. J. 36:587-593.

Varadachari, C., T. Chattopadhyay, and K. Ghosh. 1997. Complexation of humic substances with oxides of iron and aluminum. Soil Sci. 162:28-34.

Vaughan, D.J., and J.A. Tossell. 1973. Molecular orbital calculations on beryllium and boron oxyanions: interpretation of X-ray emission, ESCA, and NQR spectra and of the geochemistry of beryllium and boron. Am. Mineral. 58:765-770.

Wijnja, H., and C.P. Schulthess. 2000. Interaction of carbonate and organic anions with sulfate and selenate adsorption on an aluminum oxide. Soil Sci. Soc. Am. J. 64:898-908.

Wijnja, H., and C.P. Schulthess. 2002. Effect of carbonate on adsorption of selenate and sulfate on goethite. Soil Sci. Soc. Am. J. 66:1190-1197.

Wild, A., and A. Mazaheri. 1979. Prediction of the leaching rate of boric acid under field conditions. Geoderma 22:127-136.

Woodruff, J.R., F.W. Moore, and H.L. Musen. 1987. Potassium, boron, nitrogen and lime effects on corn yield and earleaf nutrient concentrations. Agron. J. 79:520-524.

Xu, J.M., K. Wang, R.W. Bell, Y.A. Yang, and L.B. Huang. 2001. Soil boron fractions and their relationship to soil properties. Soil Sci. Soc. Am. J. 65:133-138.

Yamauchi, S., and S. Doi. 2003. Raman spectroscopic study on the behavior of boric acid in wood. J. Wood Sci. 49:227-234.

Yano, T., N. Kunimine, S. Shibata, and M. Yamane. 2003. Structural investigation of sodium borate glasses and melts by Raman spectroscopy. I. Quantitative evaluation of structural units. Journal of Non-Crystalline Solids 321:137-146.

Yermiyahu, U., R. Keren, and Y. Chen. 1988. Boron sorption on composted organic matter. Soil Sci. Soc. Am. J. 52:1309-1313.

Yermiyahu, U., R. Keren, and Y. Chen. 1995. Boron sorption by soil in the presence of composted organic matter. Soil Sci. Soc. Am. J. 59:405-409.

APPENDIX A

DISCUSSION ON POST EDGE REGION

Background normalization was done to allow for better quantitative analysis in the absorption edge region (from 193-195 eV), where the spectra had less noise. Quantitative analysis and statements on tetrahedral $B(OH)_4^-$ complexes have been limited to relative terms proportional to trigonal $B(OH)_3$ complexes due to poor normalization in the post edge region (between 210 and 215 eV).

The spectra included in this appendix are the expanded view of peak 'b' and 'c' for Figure 4.4 and 4.5. Overall, the TEY and FY-XANES spectra for pH 7 and 9.2 showed a much more intense peak 'c' for the sample adsorbed on am-$Al(OH)_3$ under N_2. This trend validates the conclusion that more trigonal $B(OH)_3$ complexes were adsorbed on am-$Al(OH)_3$ under N_2 environment. On the other hand, the TEY and FY-XANES spectra at pH 7 (Figure A1 and A3, respectively) showed a larger peak 'b' for HA coated samples under N_2, which indicates more tetrahedral $B(OH)_4^-$ were adsorbed under those specific conditions.

In general, only qualitative analysis can be made for peak 'b' and 'c' due to the poor normalization in the post edge region. Peak 'b', characteristic of tetrahedrally coordinated B, was noticeably higher for HA coated samples, while peak 'c' characteristic of trigonally coordinated B was visibly higher for pure am-$Al(OH)_3$ samples under N_2.

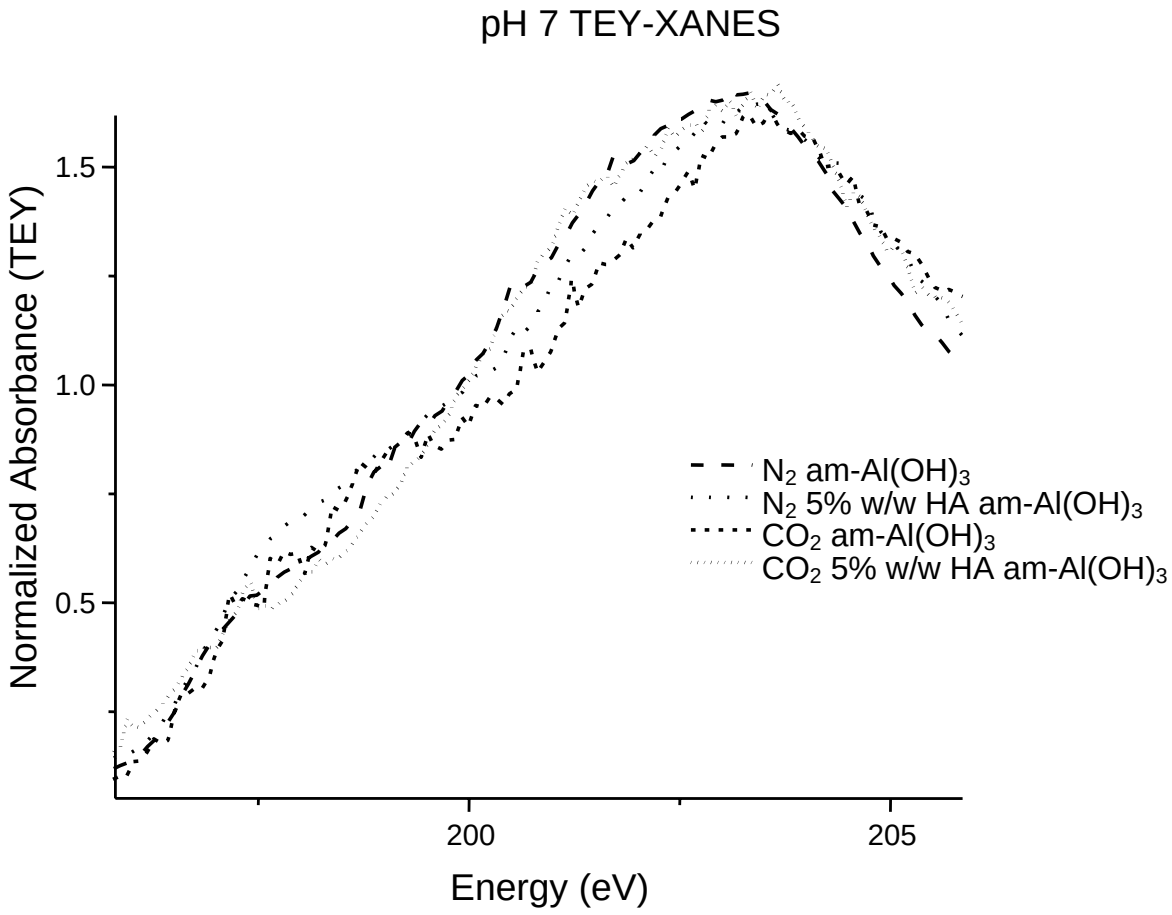

Figure. A 1 B *K*-edge pH 7 TEY-XANES spectra of boric acid adsorption isotherm samples. Expanded view of peak 'b' and 'c'. Detailed sample information and loading rate are provided in Table 4.2.

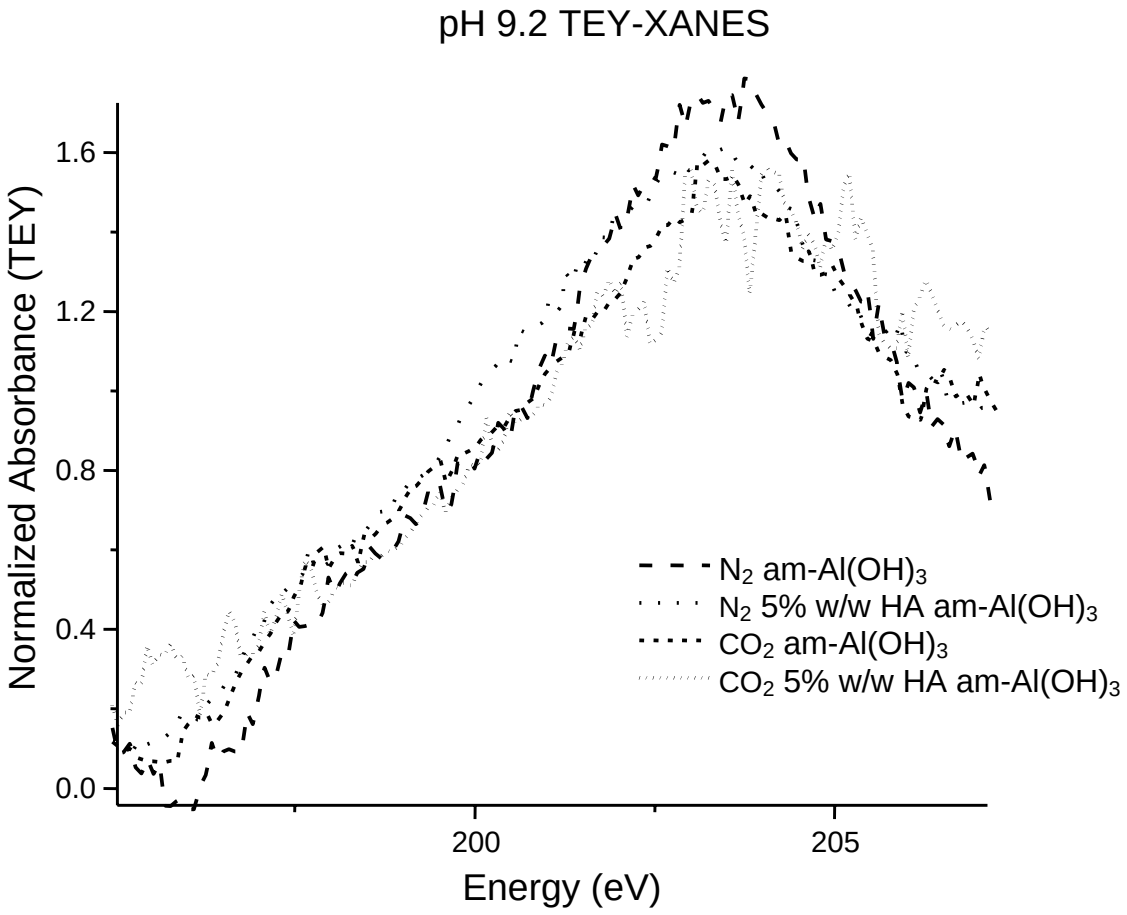

Figure. A 2 B *K*-edge pH 9.2 TEY-XANES spectra of boric acid adsorption isotherm samples. Expanded view of peak 'b' and 'c'. Detailed sample information and loading rate are provided in Table 4.2.

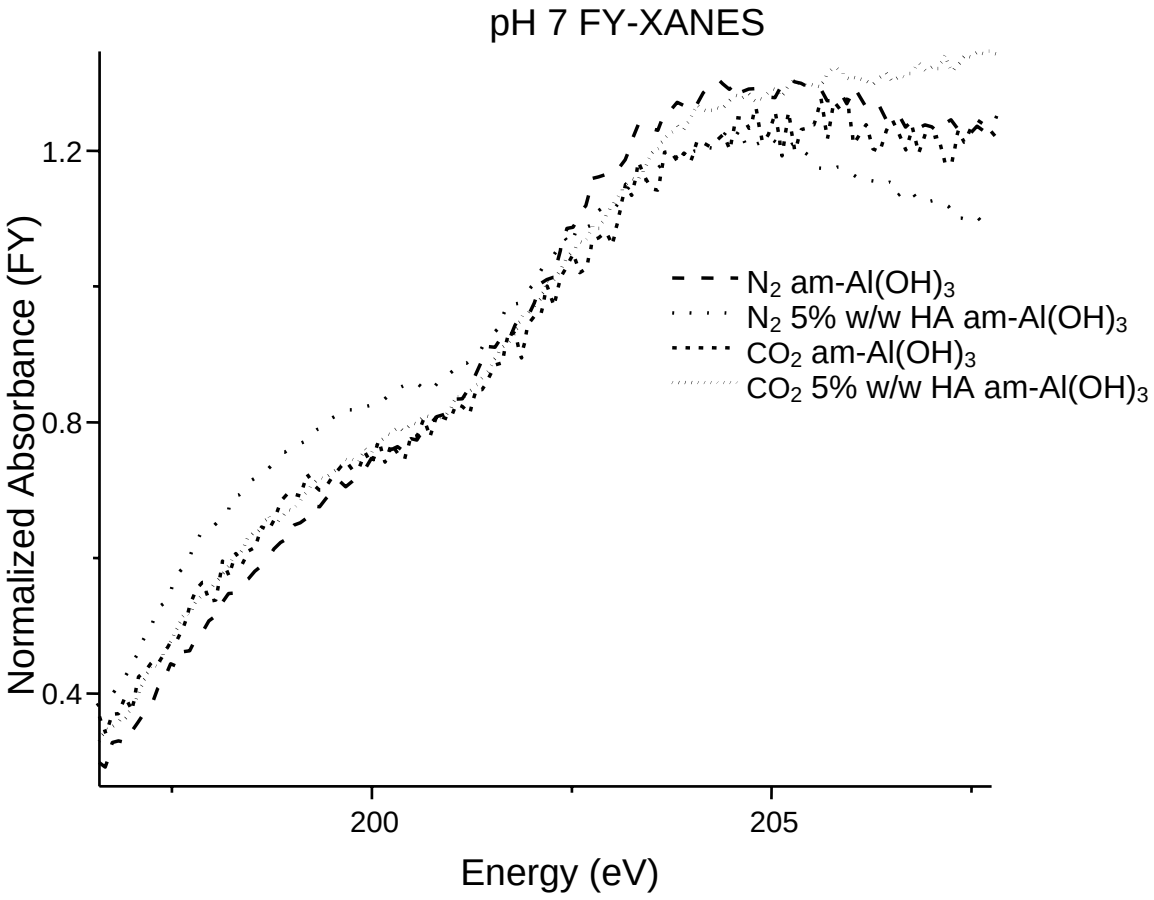

Figure. A 3 B *K*-edge pH 7 FY-XANES spectra of boric acid adsorption isotherm samples. Expanded view of peak 'b' and 'c'. Detailed sample information and loading rate are provided in Table 4.2.

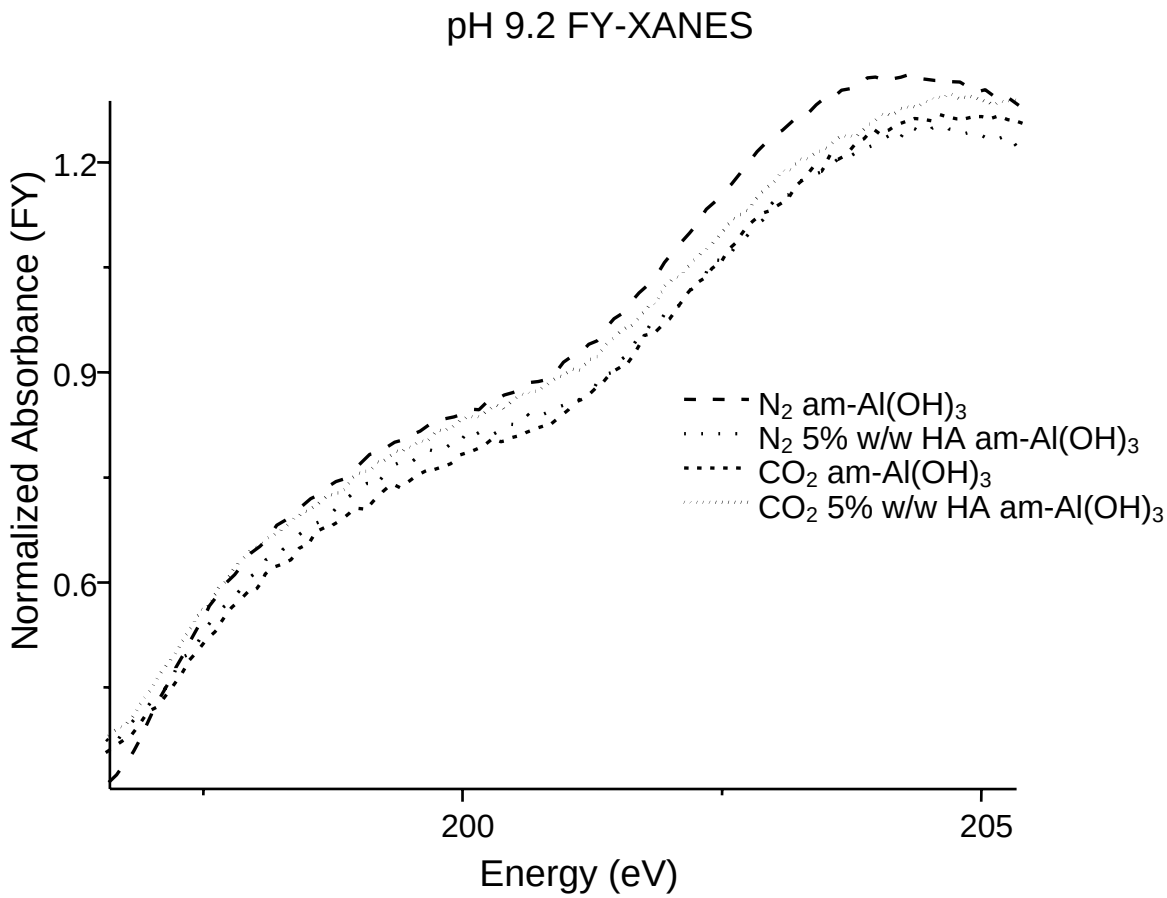

Figure. A 4 B *K*-edge pH 9.2 FY-XANES spectra of boric acid adsorption isotherm samples. Expanded view of peak 'b' and 'c'. Detailed sample information and loading rate are provided in Table 4.2.